

Supplementary Materials: Direct Control of Spin Distribution and Anisotropy in Cu-Dithiolene Complex Anions by Light

Hiroki Noma, Keishi Ohara and Toshio Naito

1. X-Ray Structural Analyses

Table S1. Crystal data of 1–3 ^a.

Compounds	1 [68]	2	3
<i>T</i> /K		296	
Crystal system		Monoclinic	
Space group	<i>P</i> 2 ₁ / <i>c</i> (#14)	<i>P</i> 2 ₁ / <i>n</i> (#14)	<i>P</i> 2 ₁ / <i>n</i> (#14)
<i>a</i> /Å	8.4655(2)	12.0835(3)	14.4217(5)
<i>b</i> /Å	14.8292(3)	13.1842(3)	17.1432(7)
<i>c</i> /Å	19.4640(4)	18.6874(4)	17.7784(7)
β /°	96.2900(7)	95.9874(7)	110.417(2)
<i>V</i> /Å ³	2428.72(8)	2960.9(1)	4119.3(3)
Z value	2	4	4
Formula	C ₃₈ H ₇₂ CuN ₂ S ₁₀	C ₂₀ H ₂₉ CuN ₅ S ₁₀	C ₄₀ H ₂₆ CuN ₄ OS ₁₀
<i>M</i> /g mol ⁻¹	941.15	723.63	962.82
<i>D</i> _{calc} /g cm ⁻³	1.287	1.623	1.552
CCDC deposit #	991696	1037127	1037129
<i>T</i> /K		100	
Crystal system		Monoclinic	
Space group	<i>P</i> 2 ₁ / <i>c</i> (#14)	<i>P</i> 2 ₁ / <i>n</i> (#14)	<i>P</i> 2 ₁ / <i>n</i> (#14)
<i>a</i> /Å	8.4012(2)	12.0063(4)	14.2959(9)
<i>b</i> /Å	14.6546(3)	12.9716(5)	16.988(1)
<i>c</i> /Å	19.2114(4)	18.6391(7)	17.746(1)
β /°	97.225(7)	95.912(7)	110.606(8)
<i>V</i> /Å ³	2346.45(9)	2887.4(2)	4033.9(5)
Z value	2	4	4
Formula	C ₃₈ H ₇₂ CuN ₂ S ₁₀	C ₂₀ H ₂₉ CuN ₅ S ₁₀	C ₄₀ H ₂₆ CuN ₄ OS ₁₀
<i>M</i> /g mol ⁻¹	941.15	723.63	962.82
<i>D</i> _{calc} /g cm ⁻³	1.332	1.664	1.585
CCDC deposit #	994604	1037128	991697

^a 1 = (*n*Bu₄N)₂[Cu(dmit)₂], 2 = [(DABCO)H⁺]₂[Cu(dmit)₂]CH₃CN, 3 = BP₂DBF[Cu(dmit)₂].

2. Band Calculation

Using the atomic parameters obtained from the X-ray structural analysis of 1–3, the molecular orbital calculation was carried out based on an extended Hückel approximation using a free program package, Caesar (vers. 1.0 and 2.0, PrimeColor Software, Raleigh, NC, USA). All of the atoms of cations and anions of 1–3 are taken into consideration in order to check if there is any cation–anion interaction, *i.e.*, band mixing. The parameters of atomic orbitals used in the calculation are tabulated in Table S2. Among the choice of some parameters' sets, they are selected on the basis that the resultant band structure can best explain the observed physical properties.

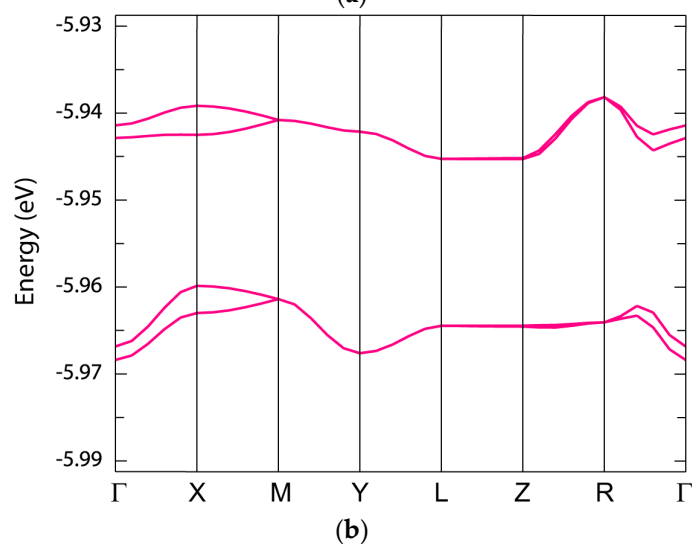
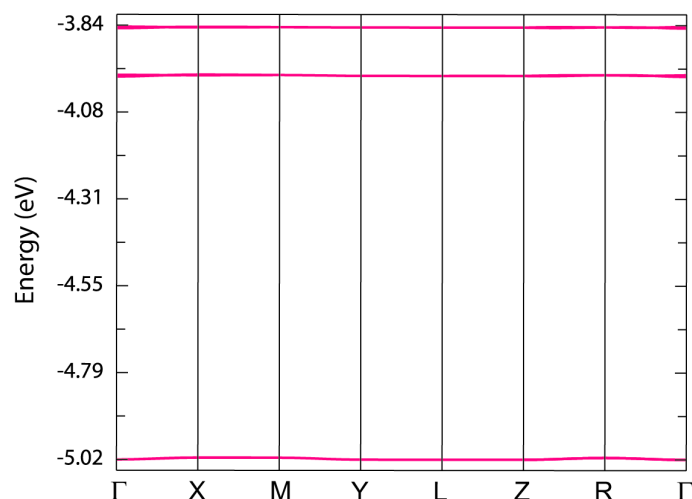
Table S2. H_{ii} and ζ used in band calculation ^a.

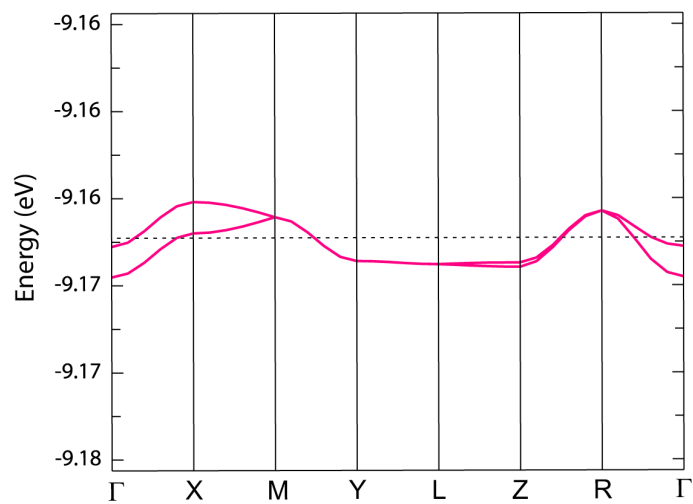
Atom	Atomic Orbital	H_{ii} (eV)	ζ_1	Coeff. 1 ^b	ζ_2	Coeff. 2 ^b
Cu	4s	-11.4	2.200	1.0000		
	4p	-6.06	2.200	1.0000		
	3d	-14.0	5.950	0.5933	2.30	0.5744
S	3s	-20.0	2.662	0.5564	1.688	0.4873
	3p	-13.3	2.338	0.5212	1.333	0.5443
C	2s	-21.4	1.831	0.7616	1.153	0.2630
	2p	-11.4	2.730	0.2595	1.257	0.8025
N	2s	-26.0	1.950	1.0000		
	2p	-13.4	1.950	1.0000		
O	2s	-32.3	2.275	1.0000		
	2p	-14.8	2.275	1.0000		
H	1s	-13.6	1.300	1.0000		

^a $H_{ii} = -\text{VSIP}$ (valence-state ionization potential (eV)). The double-zeta (for Cu 3d, S 3s, S 3p, C 2s and C 2p) or single-zeta (for the remaining orbitals) Slater type orbitals (STOs) are used;
 $\chi_{\mu}(r, \theta, \phi) \propto r^{n-1} \exp(-\zeta r) Y(\theta, \phi)$ (single-zeta STO).

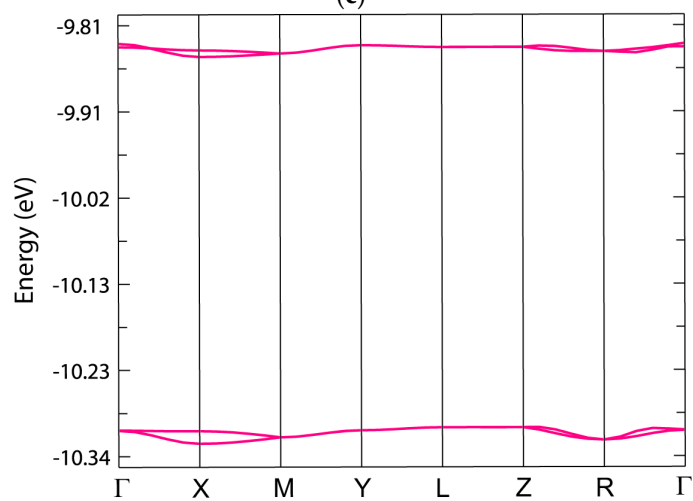
$\chi_{\mu}(r, \theta, \phi) \propto r^{n-1} [c_1 \exp(-\zeta_1 r) + c_2 \exp(-\zeta_2 r)] Y(\theta, \phi)$ (double-zeta STO);

^b Coeff. 1 and Coeff. 2 correspond to 1 and 0 in single-zeta STO, and c_1 and c_2 in double-zeta STO, respectively.

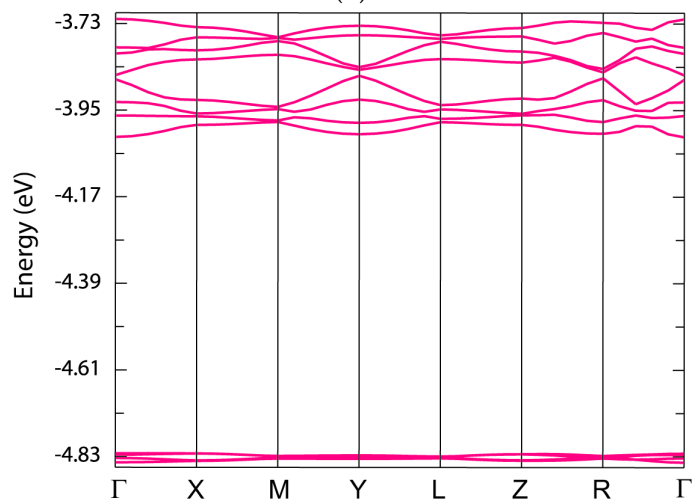




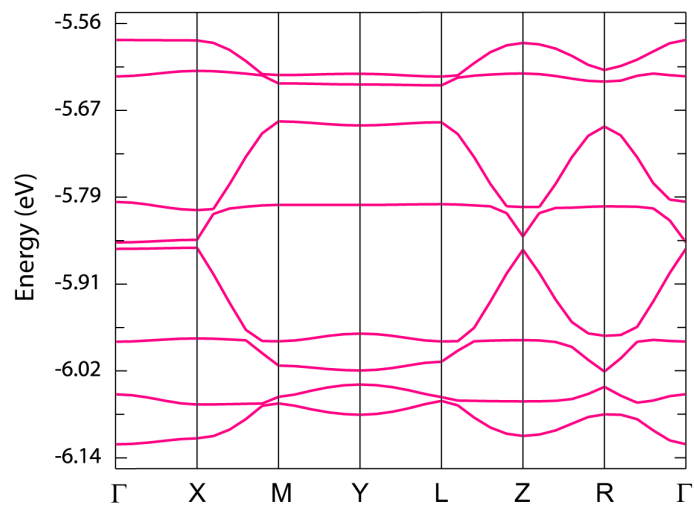
(c)



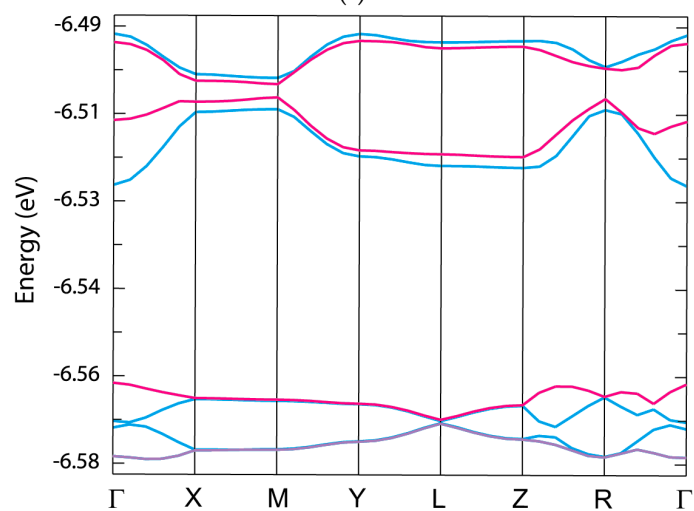
(d)



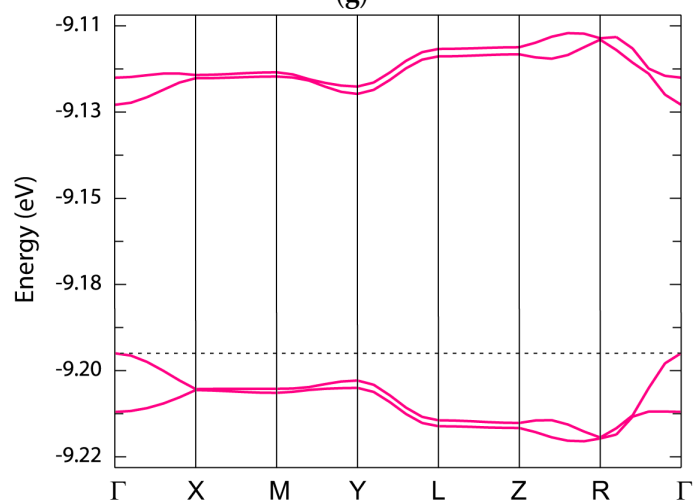
(e)



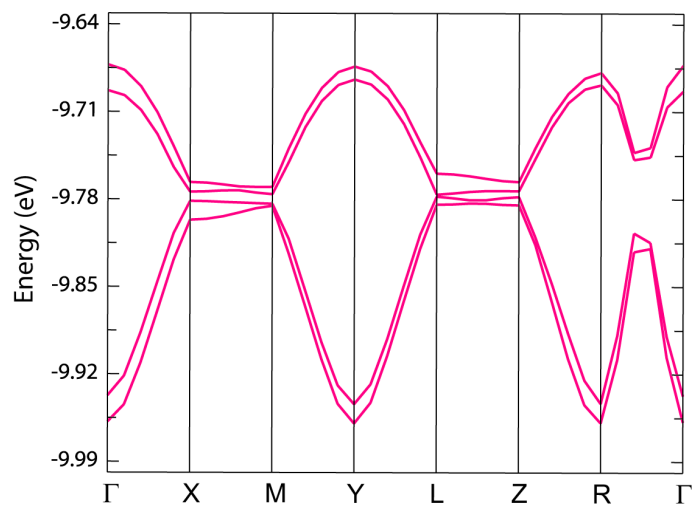
(f)



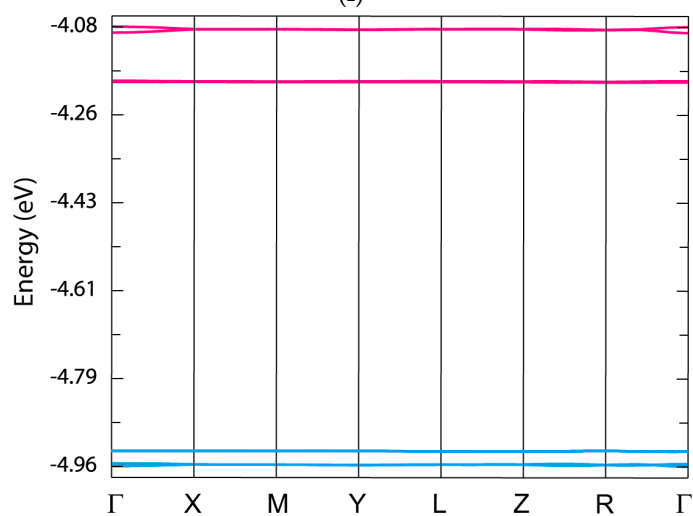
(g)



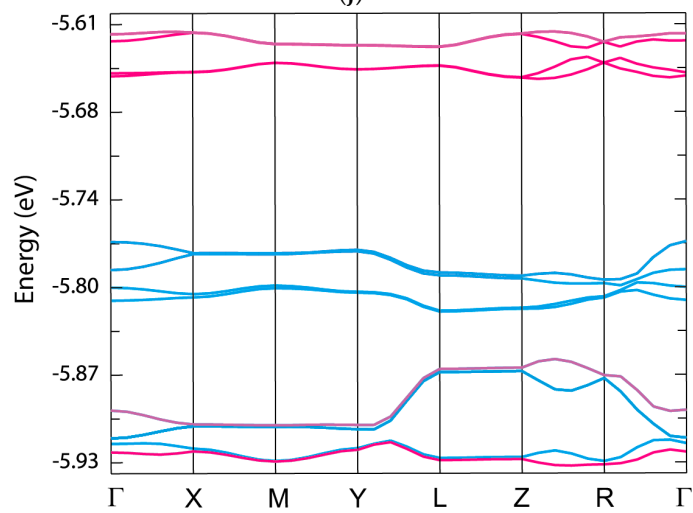
(h)



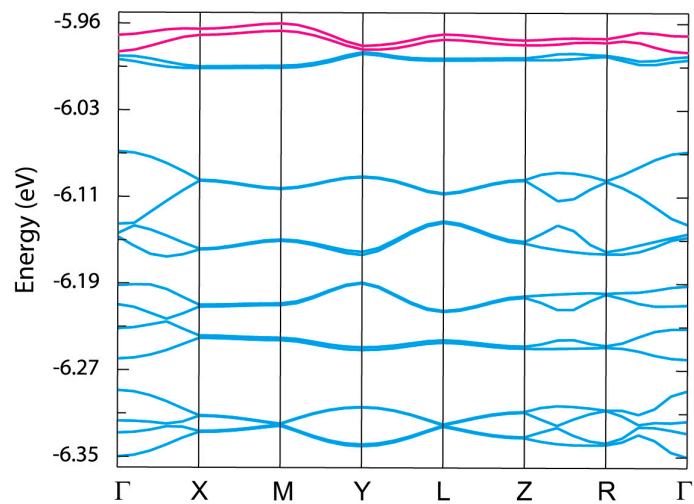
(i)



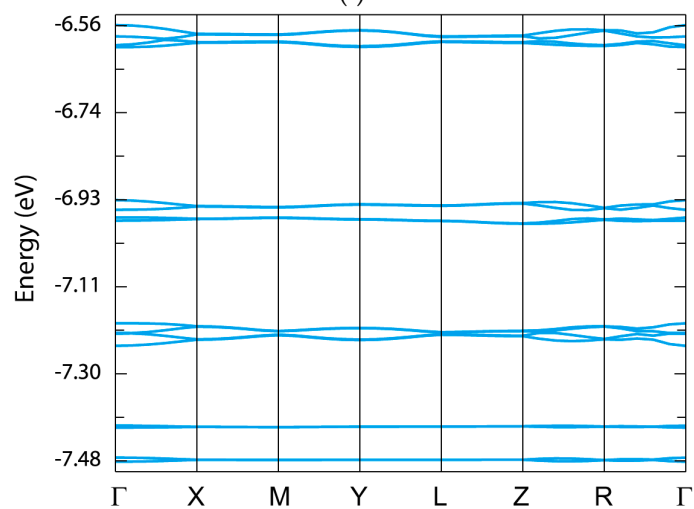
(j)



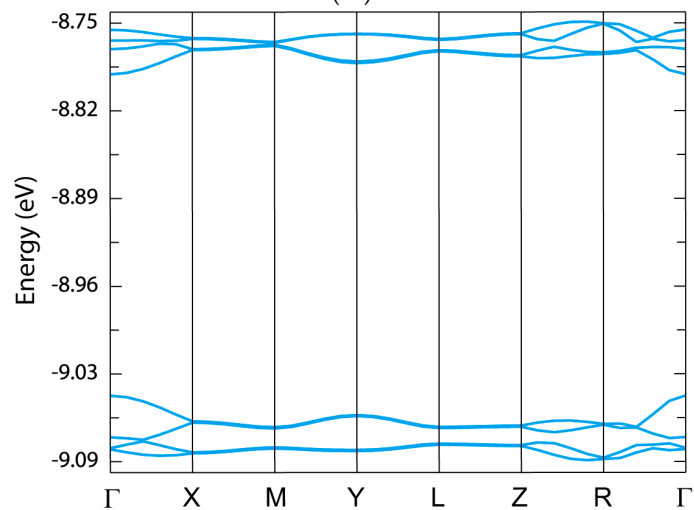
(k)



(l)



(m)



(n)

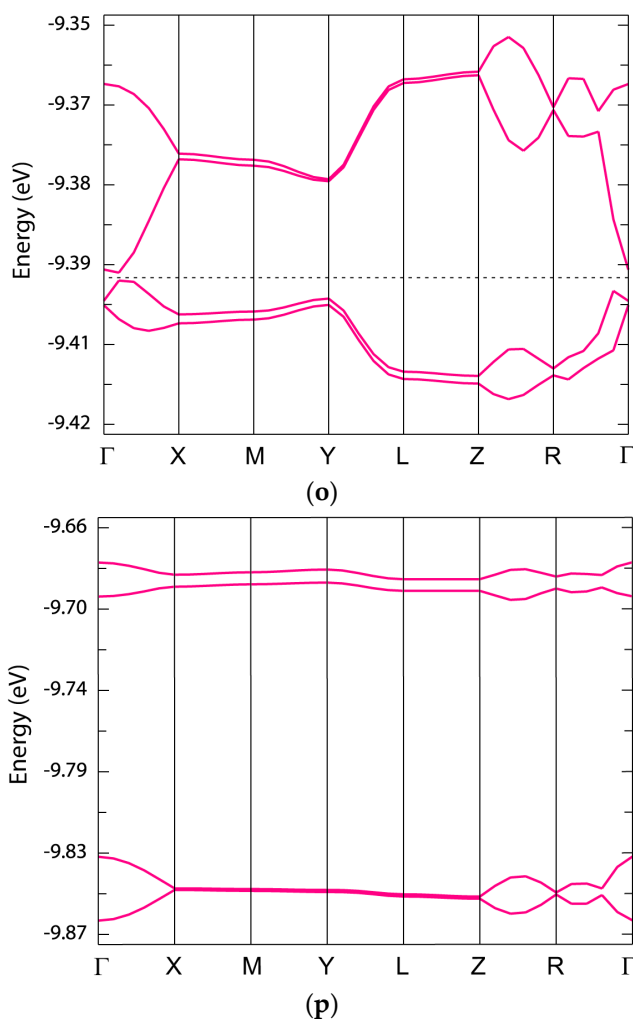


Figure S1. (a) Calculated energy bands for **1** from #311–#316. Relative contributions from $n\text{Bu}_4\text{N}^+$ (TBA^+) and $[\text{Cu}(\text{dmit})_2]^{2-}$ in each band are visually described by mixing of two colors of cyan (TBA^+) and magenta ($[\text{Cu}(\text{dmit})_2]^{2-}$) with calculated band mixing ratio. Γ , X, M, Y, L, Z and R designate the following points in the reciprocal space (0,0,0), (0.5,0,0), (0.5,0.5,0), (0,0.5,0), (0,0.5,0.5), (0,0,0.5) and (0.5,0.5,0.5), respectively; (b) calculated energy bands for **1** from #307–#310; (c) calculated energy bands for **1** from #305–#306. The broken line indicates the Fermi level. Although the Fermi level lies in the middle of the two bands, the poor band dispersion and narrow band widths suggest that **1** should be an insulator; (d) calculated energy bands for **1** from #301–#304; (e) calculated energy bands for **2** from #429–#440. Relative contributions from $(\text{DABCO})\text{H}^+$ and $[\text{Cu}(\text{dmit})_2]^{2-}$ in each band are visually described by mixing of two colors of cyan ($(\text{DABCO})\text{H}^+$) and magenta ($[\text{Cu}(\text{dmit})_2]^{2-}$) with the calculated band mixing ratio. Γ , X, M, Y, L, Z and R designate the following points in the reciprocal space (0,0,0), (0.5,0,0), (0.5,0.5,0), (0,0.5,0), (0,0.5,0.5), (0,0,0.5) and (0.5,0.5,0.5), respectively; (f) calculated energy bands for **2** from #421–#428; (g) calculated energy bands for **2** from #413–#420; (h) calculated energy bands for **2** from #409–#412. The broken line indicates the Fermi level. The band dispersion and widths, as well as Fermi level suggest that **2** should be a band insulator; (i) calculated energy bands for **2** from #405–#408; (j) calculated energy bands for **3** from #621–#628. Relative contributions from $\text{BP}_2\text{DBF}^{2+}$ and $[\text{Cu}(\text{dmit})_2]^{2-}$ in each band are visually described by the mixing of two colors of cyan ($\text{BP}_2\text{DBF}^{2+}$) and magenta ($[\text{Cu}(\text{dmit})_2]^{2-}$) with calculated band mixing ratio. Γ , X, M, Y, L, Z and R designate the following points in the reciprocal space (0,0,0), (0.5,0,0), (0.5,0.5,0), (0,0.5,0), (0,0.5,0.5), (0,0,0.5) and (0.5,0.5,0.5), respectively; (k) calculated energy bands for **3** from #609–#620; (l) calculated energy bands for **3** from #593–#608; (m) calculated energy bands for **3** from #577–#592; (n) calculated energy bands for **3** from #569–#576; (o) calculated energy bands for **3** from #565–#568. The broken line indicates the Fermi level. The band dispersion and widths, as well as Fermi level suggest that **3** should be a band insulator; (p) calculated energy bands for **3** from #561–#564.

3. ESR Spectra and Intermolecular Interactions

For the ESR spectra under UV irradiation, their ESR simulation was carried out in both isotropic and anisotropic ways, since it was considered that their isotropy could be confirmed by the comparison of both simulations. The spectra simulation was carried out using Isotropic Simulation software IsoSim/FA ver. 2.2.0 and Anisotropic Simulation software AniSim/FA ver. 2.2.0 by JEOL for isotropic and anisotropic simulations, respectively. In order to understand which spectral features originate from anisotropy, isotropic simulation was useful. Accordingly, the obtained parameters in both ways of simulation are tabulated below, though only the anisotropic one is discussed in the main text of this paper. Note that the thus obtained anisotropic parameters, such as g_x , g_y and g_z , do not have the meanings of the principal values (g_{xx} , g_{yy} , g_{zz}) corresponding to each physical property.

Table S3. Tables and figures related to ESR spectra.

Table #	Compound #	Dark/UV ^{*1}	aniso/iso ^{*2}	Dark vs. UV ^{*3}	obs. vs. sim. ^{*4}
S4	1 ($\theta = 0^\circ$)	dark	aniso	Figure 7(d)	Figure S4a
S5		UV	iso		Figure S4d
S6	2 ($\theta = 0^\circ$)	dark	aniso	Figure 7(e)	Figure S4b
S7		UV	iso		Figure S4e
S8	3 ($\theta = 45^\circ$)	dark	aniso	Figure 7(f)	Figure S4c
S9		UV	iso		Figure S4f
Table #	Compound #	dark/UV ^{*1}	aniso/iso ^{*2}	angle ϕ/g ^{*5}	obs. vs. sim. ^{*4}
S10	1			70°/min	Figure S5d
				30°/max	Figure S5e
S11	2	UV	aniso	90°/min	Figure S5f
				0°/max	Figure S5g
S12	3			0°/min	Figure S5h
				90°/max	Figure S5i

^{*1} Spectral measurement conditions. ^{*2} Spectral simulation conditions. ^{*3} Figures showing comparison between dark and UV spectra. ^{*4} Figures showing comparison between observed and simulated spectra. ^{*5} Magnetic-field-angle ϕ shown in Figure S8 and whether g -values take the minimum or maximum at the angle.

Table S4. Best parameters for anisotropic (I; Figure 7d and Figure S4a) and isotropic (II; Figure 7d and Figure S4d) reproductions of ESR spectra for $(n\text{Bu}_4\text{N})_2[\text{Cu}(\text{dmit})_2]$ (**1**) ($\theta = 0^\circ$) under the dark condition (123 K) ^a.

(I)	#1 ^b	#2 ^b
I_{rel} (%)	9	91
I	$\frac{3}{2}$ ($^{63}\text{Cu}, ^{65}\text{Cu}$)	0 ($^{12}\text{C}, ^{32}\text{S}$)
g_x	2.023	2.023
g_y	2.023	2.023
g_z	2.023	2.023
A_x (mT)	0.500	0
A_y (mT)	0.100	0
A_z (mT)	0.500	0
Γ_x (mT)	5.00	10.0
Γ_y (mT)	5.00	10.0
Γ_z (mT)	7.00	10.0
(II)	#1 ^b	#2 ^b
I_{rel} (%)	37.5	62.5
I	$\frac{3}{2}$ ($^{63}\text{Cu}, ^{65}\text{Cu}$)	0 ($^{12}\text{C}, ^{32}\text{S}$)
g	2.0225	2.0225
A (mT)	0.500	NA
Γ (mT)	6.5	10.0
Lorentz/Gaussian	80/20	80/20

^a I_{rel} , I , g_i , A_i and Γ_i ($i = x, y, z$) designate relative intensity, nuclear spin, g -value, hyperfine coupling constant and linewidth in the i -direction, respectively, for anisotropic reproduction. I_{rel} , I , g , A and Γ designate relative intensity, nuclear spin, g -value, hyperfine coupling constant and linewidth, respectively, for isotropic reproduction. ^b #1 and #2 designate the serial numbers of the oscillators (Lorentzians for anisotropic reproduction, and Lorentzians mixed with Gaussians for isotropic reproduction) required for the reproduction of the observed spectra. It does not mean that there are such numbers of independent spins in the sample. NA: Not available, the same below.

Table S5. Best parameters for anisotropic (**I**; Figures 7d and 7g) and isotropic (**II**; Figures 7d and Figure S5a) reproductions of ESR spectra for $(n\text{Bu}_4\text{N})_2[\text{Cu}(\text{dmit})_2]$ (**1**) ($\theta = 0^\circ$) under UV irradiation (250–450 nm) (123 K) ^a.

(I)	#1 ^b	#2 ^b	#3 ^b
I_{rel} (%)		37.8	62.2
	26.5	11.3	62.2
I	$\frac{3}{2}$ ($^{63}\text{Cu}, ^{65}\text{Cu}$)	$\frac{3}{2}$ ($^{63}\text{Cu}, ^{65}\text{Cu}$)	0 ($^{12}\text{C}, ^{32}\text{S}$)
g_x	2.003	2.000	1.996
g_y	1.996	1.993	1.996
g_z	1.989	1.993	1.996
A_x (mT)	1.900	4.000	NA
A_y (mT)	0.100	1.000	NA
A_z (mT)	1.900	4.000	NA
Γ_x (mT)	0.700	0.700	1.350
Γ_y (mT)	0.200	0.300	0.010
Γ_z (mT)	0.700	0.700	1.350
(II)	#1 ^b	#2 ^b	#3 ^b
I_{rel} (%)		32.3	67.7
	18.4	13.9	67.7
I	$\frac{3}{2}$ ($^{63}\text{Cu}, ^{65}\text{Cu}$)	$\frac{3}{2}$ ($^{63}\text{Cu}, ^{65}\text{Cu}$)	0 ($^{12}\text{C}, ^{32}\text{S}$)
g	2.002	1.995	1.996
A (mT)	1.800	4.000	NA
Γ (mT)	0.800	1.000	1.200

^a I_{rel} , I , g_i , A_i and Γ_i ($i = x, y, z$) designate relative intensity, nuclear spin, g -value, hyperfine coupling constant and linewidth for the i -direction, respectively, for anisotropic reproduction. I_{rel} , I , g , A and Γ designate relative intensity, nuclear spin, g -value, hyperfine coupling constant and linewidth, respectively, for isotropic reproduction. ^b #1, #2 and #3 designate the serial numbers of the oscillators (Lorentzians) required for reproduction of the observed spectra. It does not mean that there are such numbers of independent spins in the sample.

Table S6. Best parameters for anisotropic (**I**; Figure 7e and Figure S4b) and isotropic (**II**; Figure 7e and Figure S4e) reproductions of ESR spectra for [(DABCO)H⁺]₂[Cu(dmit)₂]CH₃CN (**2**) ($\theta = 0^\circ$) under the dark condition (123 K)^a.

(I)	#1^b	#2^b	#3	#4
<i>I</i> _{rel} (%)	17	83	NA	NA
<i>I</i>	$\frac{3}{2}$ (⁶³ Cu, ⁶⁵ Cu)	0 (¹² C, ³² S)	NA	NA
<i>g</i> _x	2.022	2.022	NA	NA
<i>g</i> _y	2.022	2.022	NA	NA
<i>g</i> _z	2.022	2.022	NA	NA
<i>A</i> _x (mT)	0.500	NA	NA	NA
<i>A</i> _y (mT)	0.100	NA	NA	NA
<i>A</i> _z (mT)	0.500	NA	NA	NA
Γ _x (mT)	0.90	1.10	NA	NA
Γ _y (mT)	0.60	0.60	NA	NA
Γ _z (mT)	0.90	1.10	NA	NA
(II)	#1^b	#2^b	#3	#4
<i>I</i> _{rel} (%)	24.3	10.4	23.8	41.5
<i>I</i>	$\frac{3}{2}$ (⁶³ Cu, ⁶⁵ Cu)	$\frac{3}{2}$ (⁶³ Cu, ⁶⁵ Cu)	0 (¹² C, ³² S)	0 (¹² C, ³² S)
<i>g</i>	2.007	2.004	2.000	2.0212
<i>A</i> (mT)	1.90	3.80	NA	NA
Γ (mT)	0.60	1.20	0.48	1.00

^a *I*_{rel}, *I*, *g*_{*i*}, *A*_{*i*} and Γ _{*i*} (*i* = *x*, *y*, *z*) designate relative intensity, nuclear spin, *g*-value, hyperfine coupling constant and linewidth in the *i*-direction, respectively, for anisotropic reproduction. *I*_{rel}, *I*, *g*, *A* and Γ designate relative intensity, nuclear spin, *g*-value, hyperfine coupling constant and linewidth, respectively, for isotropic reproduction. ^b #1–#4 designate the serial numbers of the oscillators (Lorentzians) required for reproduction of the observed spectra. It does not mean that there are such numbers of independent spins in the sample.

Table S7. (a) Best parameters for anisotropic (I; Figures 7e and 7h) and isotropic (II; Figure 7e and Figure S5b) reproductions of ESR spectra for [(DABCO)H⁺]₂[Cu(dmit)₂]CH₃CN (**2**) ($\theta = 0^\circ$) under UV irradiation (250–450 nm) (123 K) ^a.

(I)	#1 ^b	#2 ^b	#3 ^b	#4 ^b
<i>I</i> _{rel} (%)	21.9	31.3	9.4	68.7
<i>I</i>	$\frac{3}{2}$ (⁶³ Cu, ⁶⁵ Cu)	$\frac{3}{2}$ (⁶³ Cu, ⁶⁵ Cu)	0 (¹² C, ³² S)	0 (¹² C, ³² S)
<i>g</i> _x	2.007	2.004	2.000	2.022
<i>g</i> _y	2.000	1.997	2.000	2.022
<i>g</i> _z	1.993	1.997	2.000	2.022
<i>A</i> _x (mT)	1.900	4.000	NA	NA
<i>A</i> _y (mT)	0.100	1.000	NA	NA
<i>A</i> _z (mT)	1.900	4.000	NA	NA
Γ _x (mT)	0.600	1.200	0.900	1.100
Γ _y (mT)	0.010	1.000	0.010	0.600
Γ _z (mT)	0.600	1.200	0.900	1.100
(II)	#1 ^b	#2 ^b	#3 ^b	#4 ^b
<i>I</i> _{rel} (%)	24.3	34.7	10.4	65.3
<i>I</i>	$\frac{3}{2}$ (⁶³ Cu, ⁶⁵ Cu)	$\frac{3}{2}$ (⁶³ Cu, ⁶⁵ Cu)	0 (¹² C, ³² S)	0 (¹² C, ³² S)
<i>g</i>	2.007	2.004	2.000	2.0212
<i>A</i> (mT)	1.90	3.80	NA	NA
Γ (mT)	0.60	1.20	0.48	1.00

^a *I*_{rel}, *I*, *g*_{*i*}, *A*_{*i*} and Γ _{*i*} (*i* = *x*, *y*, *z*) designate relative intensity, nuclear spin, *g*-value, hyperfine coupling constant and linewidth for the *i*-direction, respectively, for anisotropic reproduction. *I*_{rel}, *I*, *g*, *A* and Γ designate relative intensity, nuclear spin, *g*-value, hyperfine coupling constant and linewidth, respectively, for isotropic reproduction. ^b #1–#4 designate the serial numbers of the oscillators (Lorentzians) required for reproduction of the observed spectra. It does not mean that there are such numbers of independent spins in the sample.

Table S8. Best parameters for anisotropic (**I**; Figure 7f and Figure S4c) and isotropic (**II**; Figure 7f and Figure S4f) reproductions of ESR spectra for BP₂DBF[Cu(dmit)₂] (**3**) ($\theta = 45^\circ$) under dark condition (123 K) ^a.

(I)	#1 ^b	#2 ^b
<i>I</i> _{rel} (%)	13	87
<i>I</i>	$\frac{3}{2}$ (⁶³ Cu, ⁶⁵ Cu)	0 (¹² C, ³² S)
<i>g</i> _x	2.031	2.031
<i>g</i> _y	2.031	2.031
<i>g</i> _z	2.031	2.031
<i>A</i> _x (mT)	0.500	NA
<i>A</i> _y (mT)	0.100	NA
<i>A</i> _z (mT)	0.500	NA
Γ _x (mT)	1.20	2.40
Γ _y (mT)	1.20	1.00
Γ _z (mT)	1.20	2.40
(II)	#1 ^b	#2 ^b
<i>I</i> _{rel} (%)	17	83
Lorentz/Gauss ratio	100/0	100/0
<i>I</i>	$\frac{3}{2}$ (⁶³ Cu, ⁶⁵ Cu)	0 (¹² C, ³² S)
<i>g</i>	2.029	2.029
<i>A</i> (mT)	0.50	0
Γ (mT)	1.20	1.70

^a *I*_{rel}, *I*, *g*_{*i*}, *A*_{*i*} and Γ _{*i*} (*i* = *x*, *y*, *z*) designate relative intensity, nuclear spin, *g*-value, hyperfine coupling constant and linewidth in the *i*-direction, respectively, for anisotropic reproduction. *I*_{rel}, *I*, *g*, *A* and Γ designate relative intensity, nuclear spin, *g*-value, hyperfine coupling constant and linewidth, respectively, for isotropic reproduction. ^b #1 and #2 designate the serial numbers of the oscillators (Lorentzians) required for reproduction of the observed spectra. It does not mean that there are such numbers of independent spins in the sample.

Table S9. Best parameters for anisotropic (**I**; Figures 7f and 7i) and isotropic (**II**; Figures 7f and Figure S5c) reproduction of ESR spectra for BP₂DBF[Cu(dmit)₂] (**3**) ($\theta = 45^\circ$) under UV irradiation (250–450 nm) (123 K) ^a.

(I)	#1 ^b	#2 ^b	#3 ^b	#4 ^b
<i>I</i> _{rel} (%)	33.3		66.7	
<i>I</i>	23.4	9.9	8.19	58.5
<i>I</i>	$\frac{3}{2}$ (⁶³ Cu, ⁶⁵ Cu)	$\frac{3}{2}$ (⁶³ Cu, ⁶⁵ Cu)	1 (¹⁴ N)	0 (¹² C, ³² S)
<i>g</i> _x	2.013	2.0035	2.003	2.031
<i>g</i> _y	2.004	2.0035	2.002	2.031
<i>g</i> _z	1.996	2.0035	2.002	2.031
<i>A</i> _x (mT)	1.900	4.200	0.010	NA
<i>A</i> _y (mT)	0.080	0.900	0.010	NA
<i>A</i> _z (mT)	1.900	4.200	0.010	NA
Γ _x (mT)	0.600	1.100	1.350	2.400
Γ _y (mT)	0.010	1.800	0.010	1.000
Γ _z (mT)	0.600	1.100	1.150	2.400
(II)	#1 ^b	#2 ^b	#3 ^b	#4 ^b
<i>I</i> _{rel} (%)	38.7		61.3	
<i>I</i>	26.9	11.8	12.9	48.4
<i>I</i>	$\frac{3}{2}$ (⁶³ Cu, ⁶⁵ Cu)	$\frac{3}{2}$ (⁶³ Cu, ⁶⁵ Cu)	1 (¹⁴ N)	0 (¹² C, ³² S)
<i>g</i>	2.0050	2.0035	2.0035	2.0300
<i>A</i> (mT)	1.10	4.20	0.20	NA
Γ (mT)	0.70	1.25	0.55	2.10

^a *I*_{rel}, *I*, *g*_{*i*}, *A*_{*i*} and Γ _{*i*} (*i* = *x*, *y*, *z*) designate relative intensity, nuclear spin, *g*-value, hyperfine coupling constant and linewidth for the *i*-direction, respectively, for anisotropic reproduction. *I*_{rel}, *I*, *g*, *A* and Γ designate relative intensity, nuclear spin, *g*-value, hyperfine coupling constant and linewidth, respectively, for isotropic reproduction. ^b #1–#4 designate the serial numbers of the oscillators (Lorentzians) required for reproduction of the observed spectra. It does not mean that there are such numbers of independent spins in the sample.

Table S10. Best parameters for anisotropic reproduction of ESR spectra for $(n\text{Bu}_4\text{N})_2[\text{Cu}(\text{dmit})_2]$ (**I**) (**I** for Figure S5d ($\phi = 70^\circ$) and **II** for Figure S5e ($\phi = 30^\circ$)) under UV irradiation (250–450 nm) (123 K) ^a.

(I)	#1 ^b	#2 ^b	#3 ^b	#4
I_{rel} (%)		3.1	96.6	0.2
	0.9	2.2	96.6	0.2
I	$\frac{3}{2}$ ($^{63}\text{Cu}, ^{65}\text{Cu}$)	$\frac{3}{2}$ ($^{63}\text{Cu}, ^{65}\text{Cu}$)	0 ($^{12}\text{C}, ^{32}\text{S}$)	1 (^{14}N)
g_x	2.0060	2.0030	2.0320	2.0045
g_y	2.0036	2.0030	2.0320	2.0036
g_z	2.0036	2.0030	2.0320	2.0036
A_x (mT)	0.100	1.500	NA	0.0001
A_y (mT)	0.100	0.500	NA	0.0001
A_z (mT)	0.100	1.500	NA	0.0001
Γ_x (mT)	0.800	0.800	7.000	0.500
Γ_y (mT)	0.800	0.800	7.000	0.500
Γ_z (mT)	0.800	0.800	7.000	0.500
Lorentzian/Gaussian	70/30	80/20	80/20	70/30
(II)	#1 ^b	#2 ^b	#3 ^b	#4
I_{rel} (%)		14.1	85.1	0.7
	2.8	11.3	85.1	0.7
I	$\frac{3}{2}$ ($^{63}\text{Cu}, ^{65}\text{Cu}$)	$\frac{3}{2}$ ($^{63}\text{Cu}, ^{65}\text{Cu}$)	0 ($^{12}\text{C}, ^{32}\text{S}$)	1 (^{14}N)
g_x	2.0035	2.0035	2.0500	2.0045
g_y	2.0035	2.0035	2.0500	2.0036
g_z	2.0035	2.0035	2.0500	2.0036
A_x (mT)	0.100	1.500	NA	0.0001
A_y (mT)	0.100	0.500	NA	0.0001
A_z (mT)	0.100	1.500	NA	0.0001
Γ_x (mT)	0.800	1.100	11.500	0.500
Γ_y (mT)	0.800	1.100	11.500	0.500
Γ_z (mT)	0.800	1.100	11.500	0.500
Lorentzian/Gaussian	80/20	80/20	10/90	70/30

^a I_{rel} , I , g_i , A_i and Γ_i ($i = x, y, z$) designate relative intensity, nuclear spin, g -value, hyperfine coupling constant and linewidth for the i -direction, respectively. ^b #1–#4 designate the serial numbers of the oscillators (Lorentzians mixed with Gaussians) required for reproduction of the observed spectra. It does not mean that there are such numbers of independent spins in the sample. Oscillators #1 and #2 are for the signal from ground-state and photo-excited Cu(II) atoms, while Oscillator #3 from the dmit-ligands. Oscillator #4 is for the signal from DPPH.

Table S11. Best parameters for anisotropic reproduction of ESR spectra for [(DABCO)H⁺]₂[Cu(dmit)₂]CH₃CN (**I** for Figure S5f ($\phi = 90^\circ$) and **II** for Figure S5g ($\phi = 0^\circ$)) under UV irradiation (250–450 nm) (123 K) ^a.

(I)	#1 ^b	#2 ^b	#3 ^b	#4
<i>I</i> rel (%)		18.2	80.9	1.0
	7.3	10.9	80.9	1.0
<i>I</i>	$\frac{3}{2}$ (⁶³ Cu, ⁶⁵ Cu)	$\frac{3}{2}$ (⁶³ Cu, ⁶⁵ Cu)	0 (¹² C, ³² S)	1 (¹⁴ N)
<i>g</i> _x	2.0035	2.0030	2.0260	2.0045
<i>g</i> _y	2.0035	2.0030	2.0260	2.0036
<i>g</i> _z	2.0035	2.0030	2.0260	2.0036
<i>A</i> _x (mT)	0.100	1.500	NA	0.0001
<i>A</i> _y (mT)	0.100	0.500	NA	0.0001
<i>A</i> _z (mT)	0.100	1.500	NA	0.0001
Γ _x (mT)	1.100	0.850	1.500	0.500
Γ _y (mT)	1.100	0.850	1.500	0.500
Γ _z (mT)	1.100	0.850	1.500	0.500
Lorentzian/Gaussian	70/30	80/20	80/20	70/30
(II)	#1 ^b	#2 ^b	#3 ^b	#4
<i>I</i> rel (%)		49.0	49.0	1.9
	10.1	38.9	49.0	1.9
<i>I</i>	$\frac{3}{2}$ (⁶³ Cu, ⁶⁵ Cu)	$\frac{3}{2}$ (⁶³ Cu, ⁶⁵ Cu)	0 (¹² C, ³² S)	1 (¹⁴ N)
<i>g</i> _x	2.0035	2.0035	2.0260	2.0045
<i>g</i> _y	2.0035	2.0035	2.0260	2.0036
<i>g</i> _z	2.0035	2.0035	2.0260	2.0036
<i>A</i> _x (mT)	0.100	1.500	NA	0.0001
<i>A</i> _y (mT)	0.100	0.500	NA	0.0001
<i>A</i> _z (mT)	0.100	1.500	NA	0.0001
Γ _x (mT)	0.800	1.100	3.500	0.500
Γ _y (mT)	0.800	1.100	3.500	0.500
Γ _z (mT)	0.800	1.100	3.500	0.500
Lorentzian/Gaussian	70/30	80/20	80/20	70/30

^a *I*_{rel}, *I*, *g*_{*i*}, *A*_{*i*} and Γ _{*i*} (*i* = *x*, *y*, *z*) designate relative intensity, nuclear spin, *g*-value, hyperfine coupling constant and linewidth for the *i*-direction, respectively. ^b #1–#4 designate the serial numbers of the oscillators (Lorentzians mixed with Gaussians) required for reproduction of the observed spectra. It does not mean that there are such numbers of independent spins in the sample. Oscillators #1 and #2 are for the signal from ground-state and photo-excited Cu(II) atoms, while Oscillator #3 from the dmit-ligands. Oscillator #4 is for the signal from DPPH.

Table S12. Best parameters for anisotropic reproduction of ESR spectra for BP₂DBF[Cu(dmit)₂] (**3**) (**I** for Figure S5h ($\phi = 0^\circ$) and **II** for Figure S5i ($\phi = 90^\circ$)) under UV irradiation (250–450 nm) (123 K) ^a.

(I)	#1^b	#2^b	#3^b	#4
<i>I</i> _{rel} (%)		94.2	5.7	0.1
	21.2	73.0	5.7	0.1
<i>I</i>	$\frac{3}{2}$ (⁶³ Cu, ⁶⁵ Cu)	$\frac{3}{2}$ (⁶³ Cu, ⁶⁵ Cu)	0 (¹² C, ³² S)	1 (¹⁴ N)
<i>g</i> _x	2.0035	2.0035	2.0280	2.0045
<i>g</i> _y	2.0035	2.0035	2.0280	2.0036
<i>g</i> _z	2.0035	2.0035	2.0280	2.0036
<i>A</i> _x (mT)	0.100	1.500	NA	0.0001
<i>A</i> _y (mT)	0.100	0.500	NA	0.0001
<i>A</i> _z (mT)	0.100	1.500	NA	0.0001
Γ _x (mT)	0.800	1.100	1.400	0.500
Γ _y (mT)	0.800	1.100	1.400	0.500
Γ _z (mT)	0.800	1.100	1.400	0.500
Lorentzian/Gaussian	80/20	80/20	80/20	70/30
(II)	#1^b	#2^b	#3^b	#4
<i>I</i> _{rel} (%)		67.7	30.1	2.3
	11.3	56.4	30.1	2.3
<i>I</i>	$\frac{3}{2}$ (⁶³ Cu, ⁶⁵ Cu)	$\frac{3}{2}$ (⁶³ Cu, ⁶⁵ Cu)	0 (¹² C, ³² S)	1 (¹⁴ N)
<i>g</i> _x	2.0035	2.0035	2.0530	2.0045
<i>g</i> _y	2.0035	2.0035	2.0530	2.0036
<i>g</i> _z	2.0035	2.0035	2.0530	2.0036
<i>A</i> _x (mT)	0.100	1.500	NA	0.0001
<i>A</i> _y (mT)	0.100	0.500	NA	0.0001
<i>A</i> _z (mT)	0.100	1.500	NA	0.0001
Γ (mT)	0.800	1.100	4.500	0.500
Γ _y (mT)	0.800	1.100	4.500	0.500
Γ _z (mT)	0.800	1.100	4.500	0.500
Lorentzian/Gaussian	80/20	80/20	80/20	70/30

^a *I*_{rel}, *I*, *g*_{*i*}, *A*_{*i*} and Γ _{*i*} (*i* = *x*, *y*, *z*) designate relative intensity, nuclear spin, *g*-value, hyperfine coupling constant and linewidth for the *i*-direction, respectively. ^b #1, #2, #3 and #4 designate the serial numbers of the oscillators (Lorentzians mixed with Gaussians) required for reproduction of the observed spectra. It does not mean that there are such numbers of independent spins in the sample. Oscillators #1 and #2 are for the signal from ground-state and photo-excited Cu(II) atoms, while Oscillator #3 from the dmit-ligands. Oscillator #4 is for the signal from DPPH.

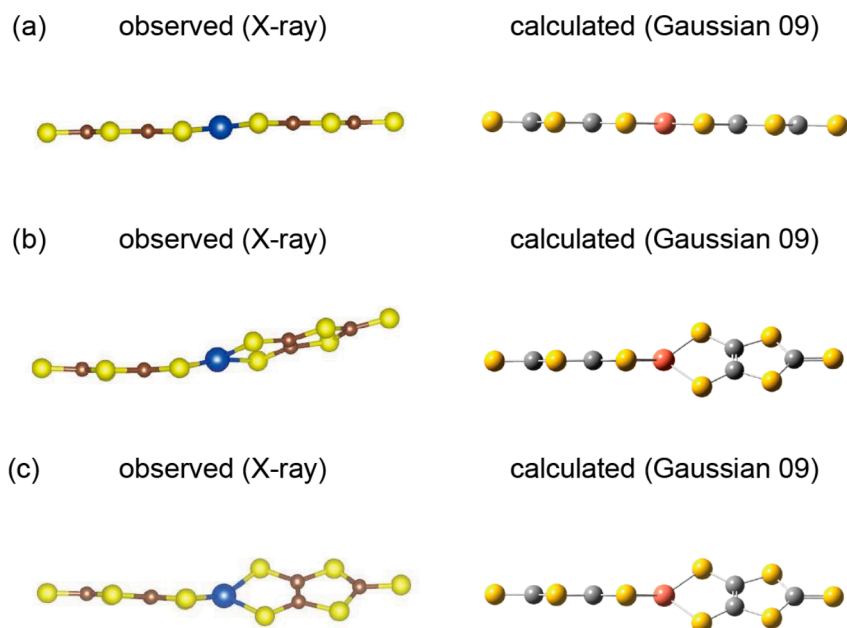


Figure S2. Comparison of molecular structures obtained from X-ray structural analysis (**left**) and those obtained from structural optimization by Gaussian 09 (**right**); (a) **1**; (b) **2**; and (c) **3**. In (a)–(c), yellow, brown, and blue spheres designate S, C, and Ni atoms, respectively in the observed structures, while yellow, grey, and orange spheres designate S, C, and Ni atoms, respectively in the calculated structures. In the calculation, the initial structures were assumed to be the respective observed structures.

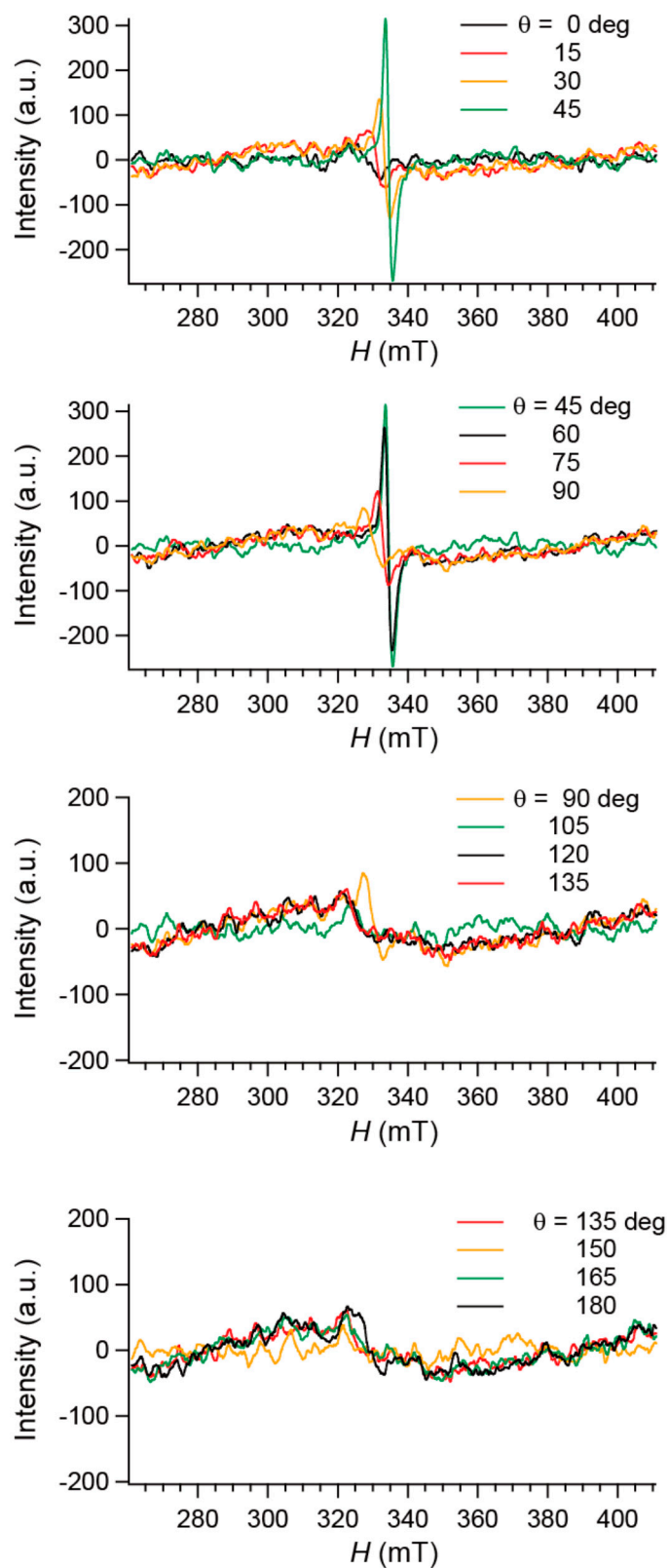
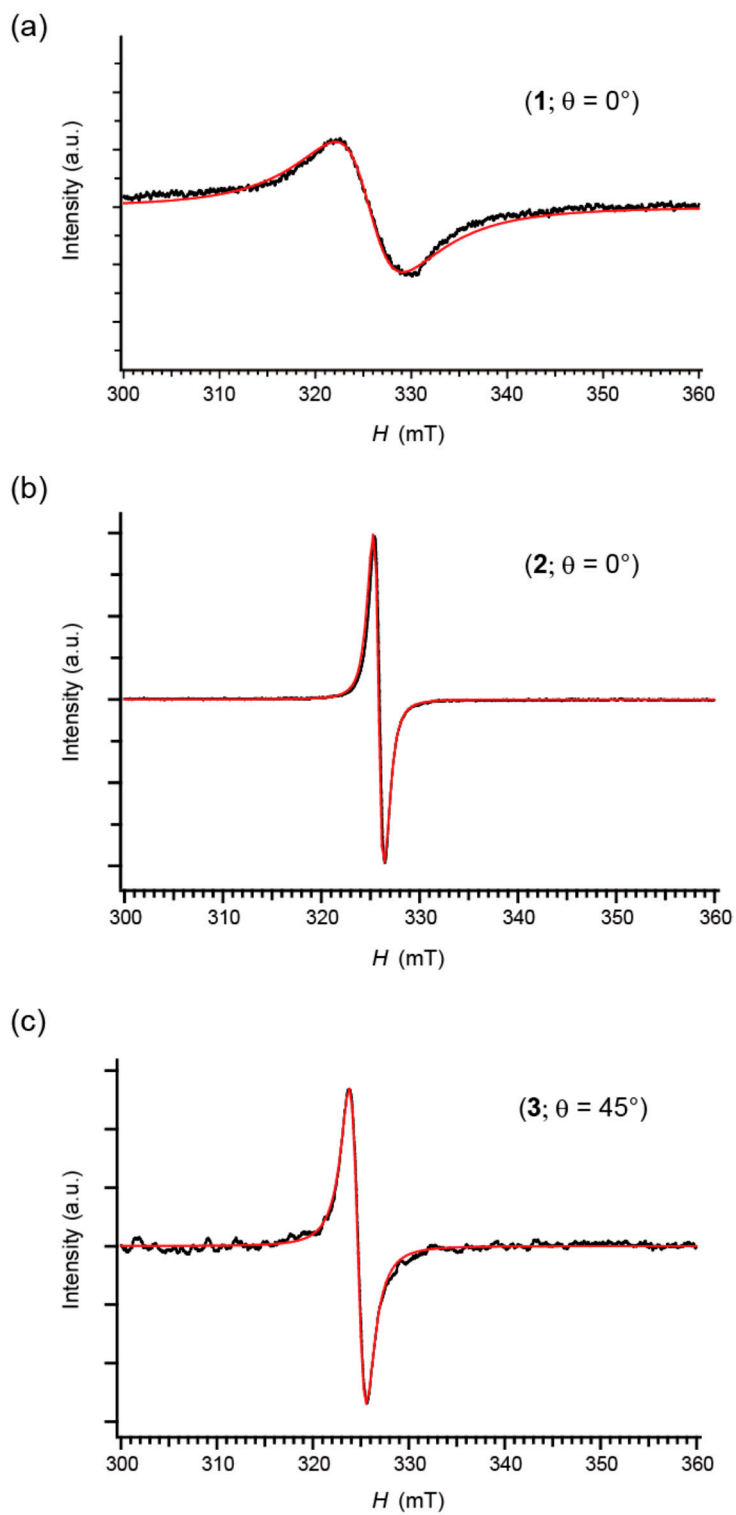


Figure S3. Angle-dependence of ESR spectra under dark condition for **3**. The angle θ defines the rotation angle around the axis normal to the bc -plane (see Figures 2e). $\theta = 0$ means $H \parallel [011]$ -direction. For comparison, the same spectra ($\theta = 45, 90$ and 135°) appear in different graphs.



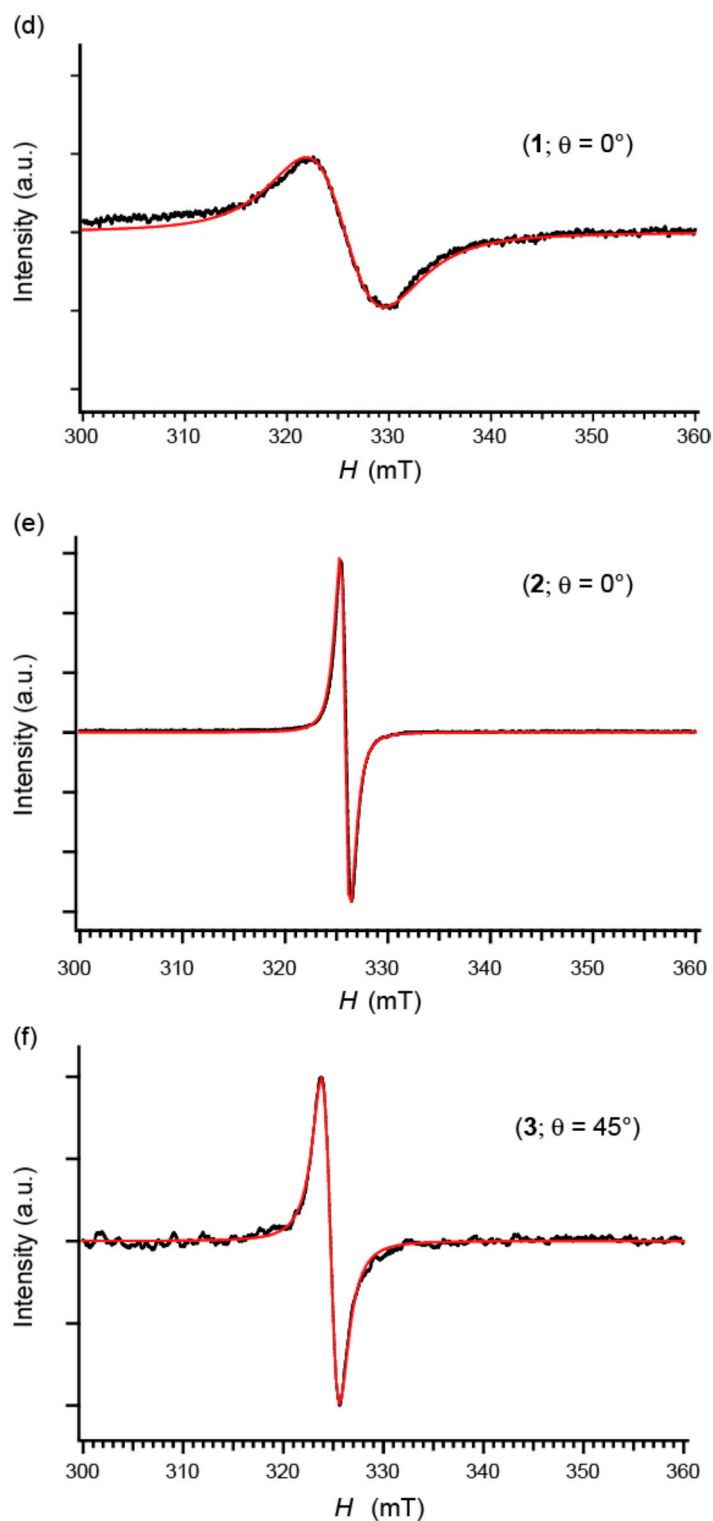
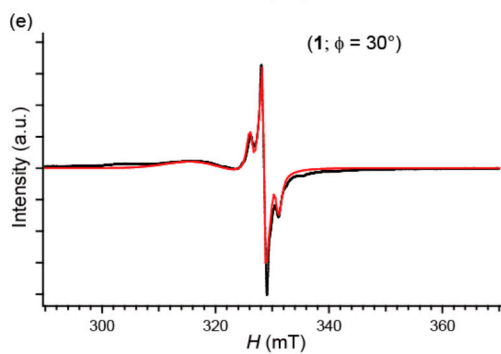
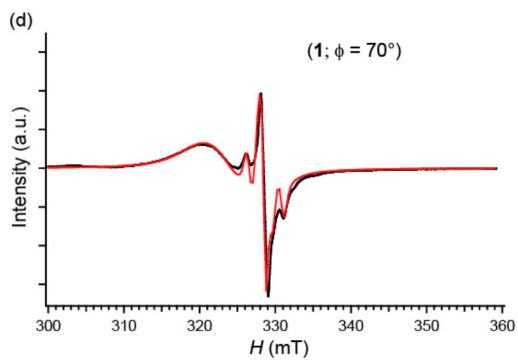
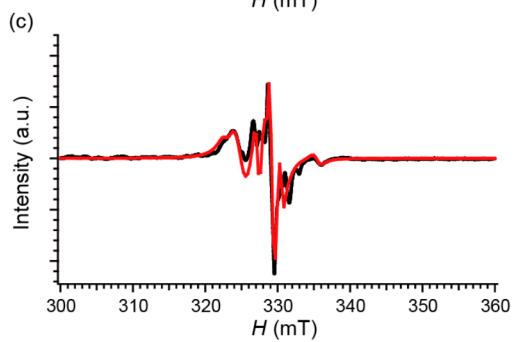
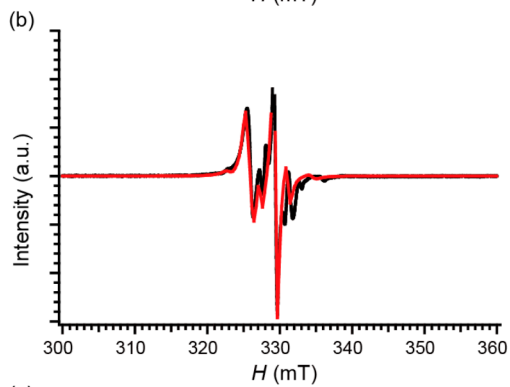
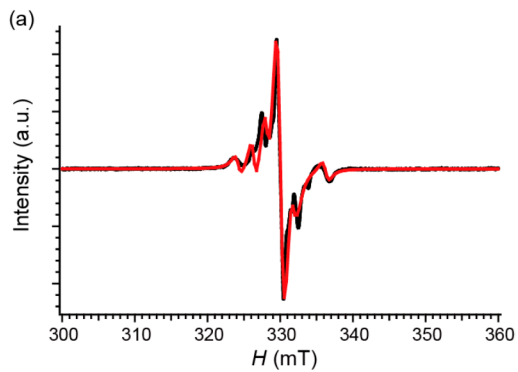


Figure S4. Comparison between observed (black) and anisotropically-simulated (red) ESR spectra under dark conditions for: (a) **1** ($\theta = 0^\circ$) [68]; (b) **2** ($\theta = 0^\circ$); and (c) **3** ($\theta = 45^\circ$). For parameters, see Tables S4, S6 and S8 for **1**, **2** and **3**, respectively. The observed spectra are the same data with those in Figure 7d–f. Comparison between observed (black) and isotropically-simulated (red) ESR spectra under dark conditions for: (d) **1** ($\theta = 0^\circ$); (e) **2** ($\theta = 0^\circ$); and (f) **3** ($\theta = 45^\circ$). For parameters, see Tables S4, S6 and S8 for **1**, **2** and **3**, respectively. The observed spectra are the same data with those in Figure 7d–f.



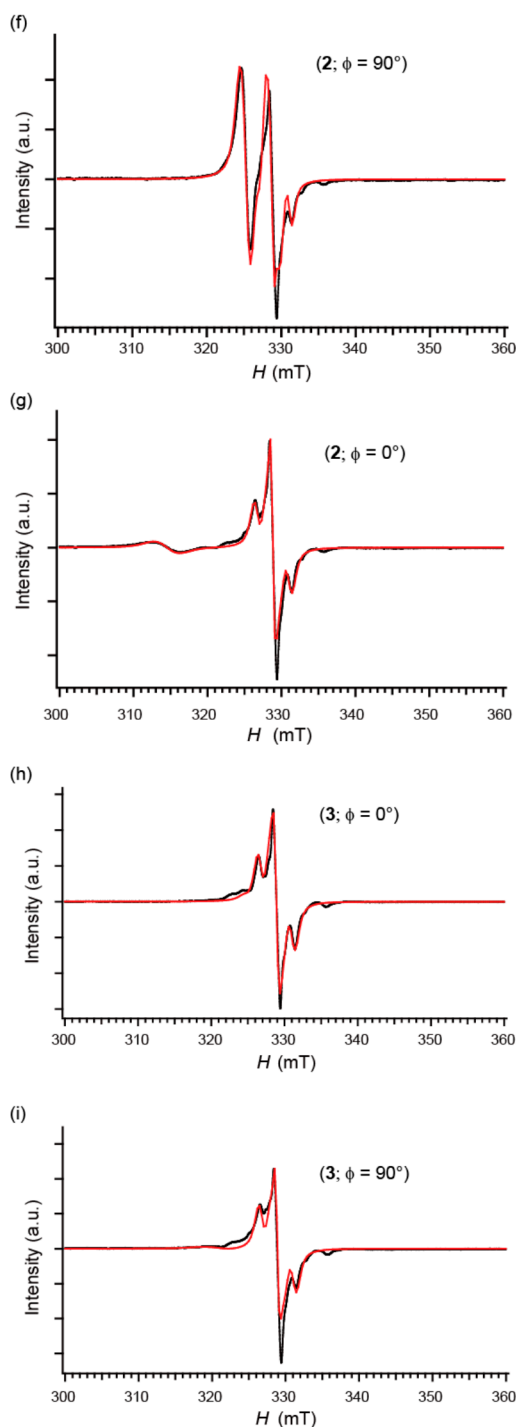


Figure S5. Comparison between observed (black) and isotropically-simulated (red) ESR spectra under UV irradiated condition for: (a) **1** ($\theta = 0^\circ$); (b) **2** ($\theta = 0^\circ$), and (c) **3** ($\theta = 45^\circ$). For parameters, see Tables S5, S7 and S9 for **1**, **2** and **3**, respectively. The observed spectra are the same data with those in Figures 7d–f. Comparison between observed (black) and anisotropically simulated (red) ESR spectra under UV irradiated condition at 123 K for **1**: (d) $\phi = 70^\circ$ and (e) $\phi = 30^\circ$. The observed spectra are the same data as those in Figures S7c,d. For the definition of angle ϕ , see Figure S8a. For the parameters, see Table S10. Comparison between observed (black) and anisotropically simulated (red) ESR spectra under UV irradiated condition at 123 K for **2**: (f) $\phi = 90^\circ$ and (g) $\phi = 0^\circ$. The observed spectra are the same data with those in Figure S7g,h. For the definition of angle ϕ , see Figure S8b. For the parameters, see Table S11. Comparison between observed (black) and anisotropically-simulated (red) ESR spectra under UV irradiated condition at 123 K for **3**: (h) $\phi = 0^\circ$ and (i) $\phi = 90^\circ$. The observed spectra are the same data with those in Figures S7k,l. For the definition of angle ϕ , see Figure S8c. For the parameters, see Table S12.

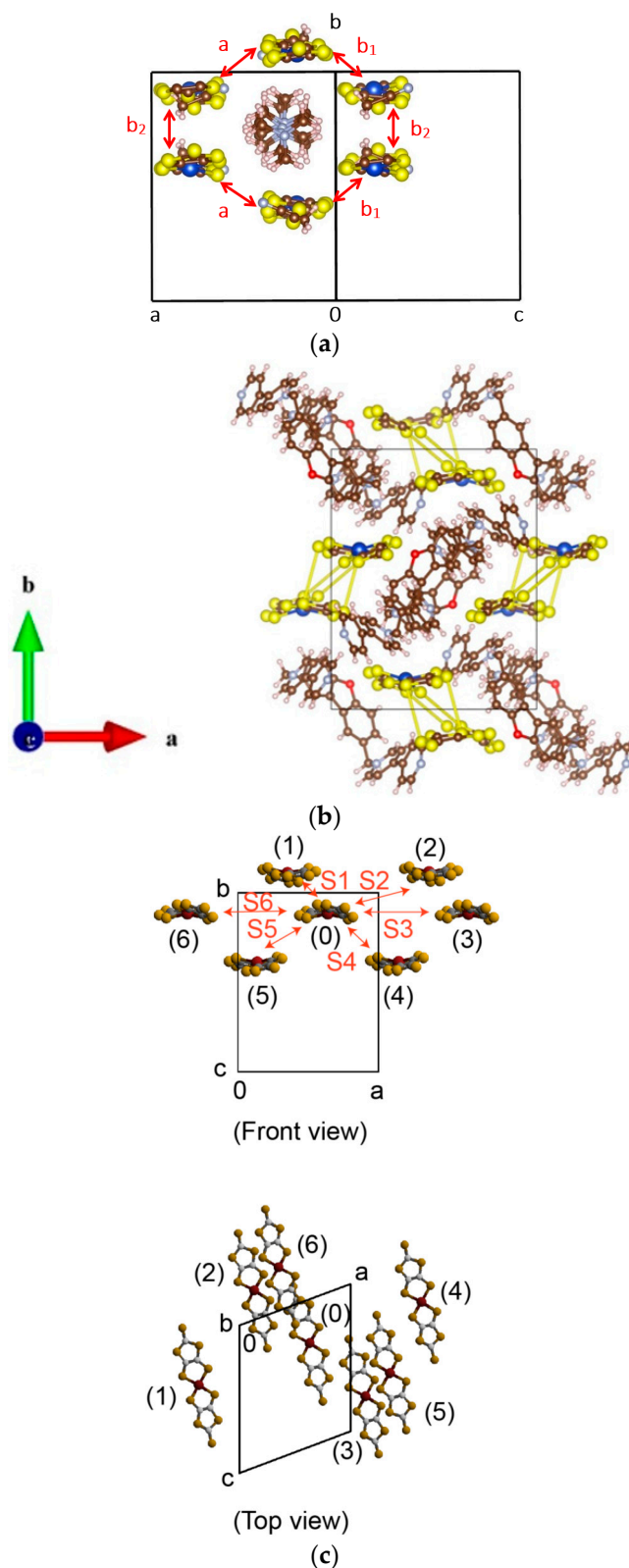
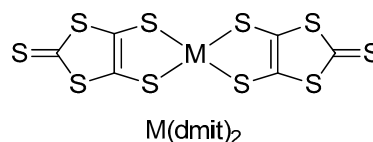
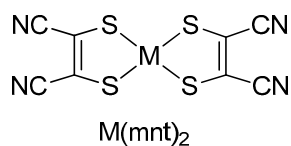


Figure S6. (a) Close up view of molecular arrangement and intermolecular interaction of $[\text{Cu}(\text{dmit})_2]^{2-}$ anions in **2**. C: brown; H: pink; N: grey; S: yellow; Cu: blue. The overlap and transfer integrals are tabulated in Table S13. (b) Molecular arrangement in the *ab*-plane of **3**; brown, yellow, red, blue, grey and pale brown spheres designate carbon, sulfur, oxygen, copper, nitrogen and hydrogen atoms, respectively. The S-S distances shorter than 4.00 Å between $[\text{Cu}(\text{dmit})_2]^{2-}$ are connected by yellow solid lines. (c) Close up view of molecular arrangement and intermolecular interaction of $[\text{Cu}(\text{dmit})_2]^{2-}$ anions in **3**. The overlap and transfer integrals are tabulated in Table S13.

Table S13. Overlap (S) and transfer (H_{ij}) integrals calculated by extended Hückel method for **2** and **3**.

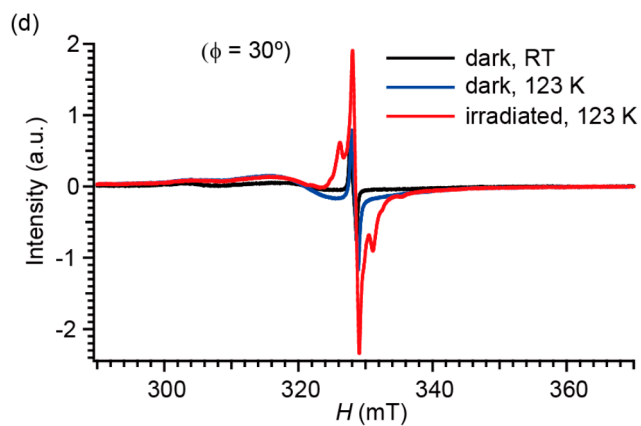
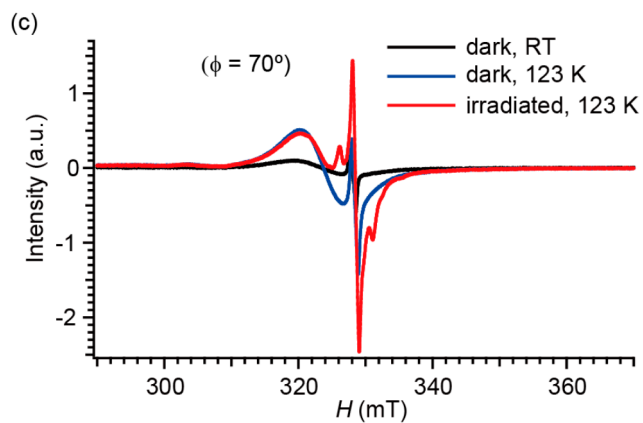
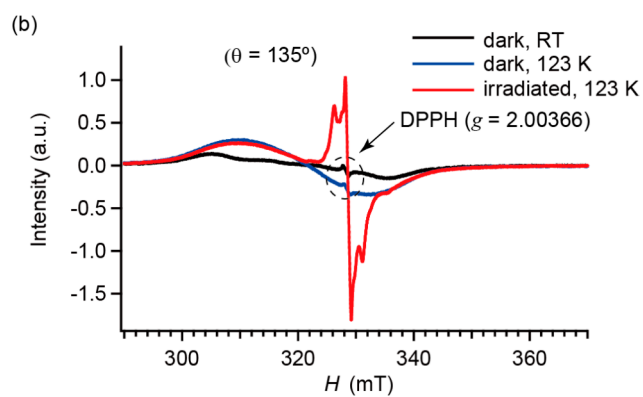
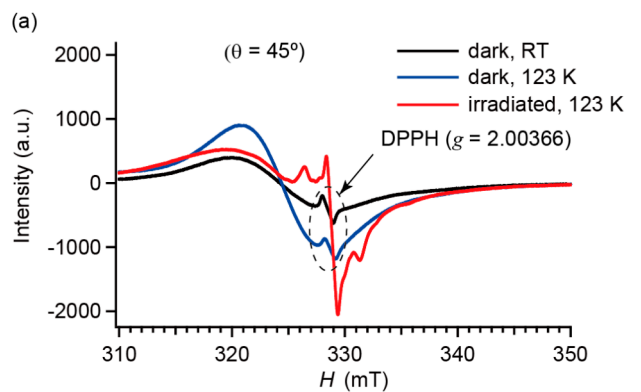
Compounds	Interacting Molecular Pair ¹	$S \times 10^3$	H_{ij} (meV)
2	a	-4.5	89
	b ₁	0.3	-9
	b ₂	-0.3	61
	S1	1.5	-30.0
	S2	0	-0.1
	S3	0	0
3	S4	0.7	-13.6
	S5	-0.7	13.6
	S6	0	0

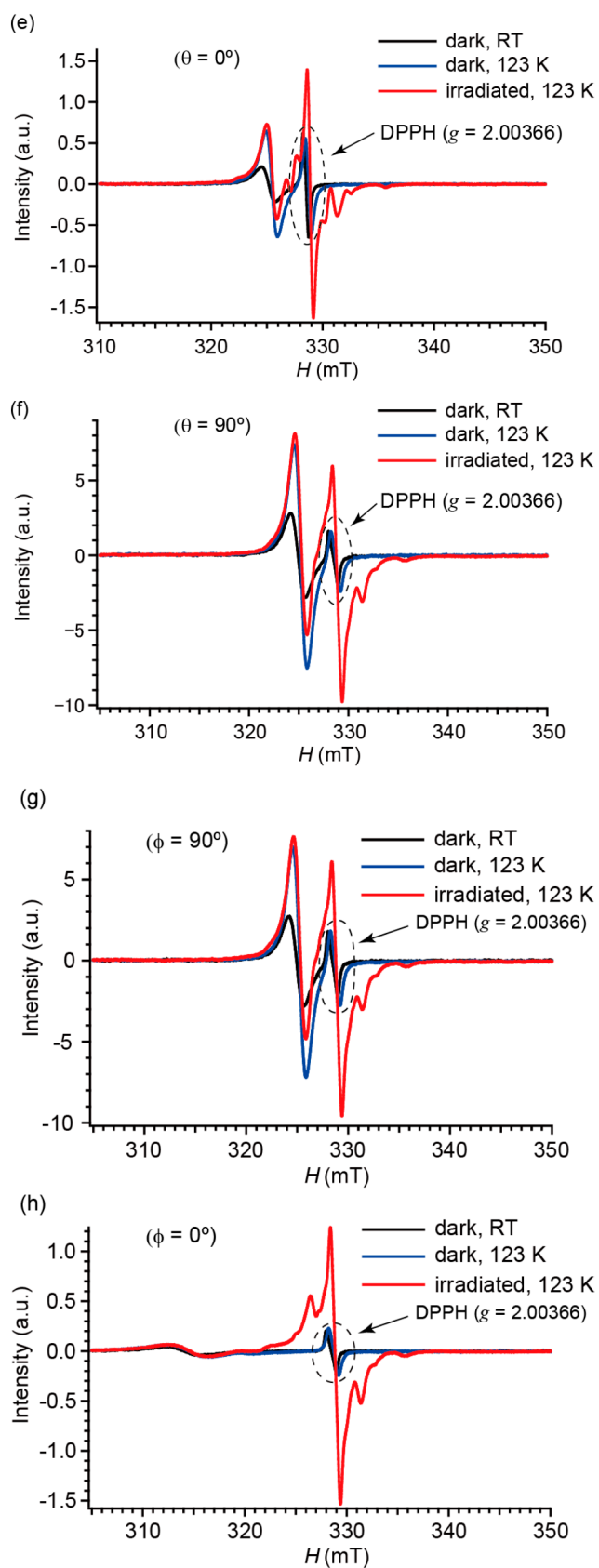
¹ See Figures S6a and S6c for **2** and **3**, respectively.

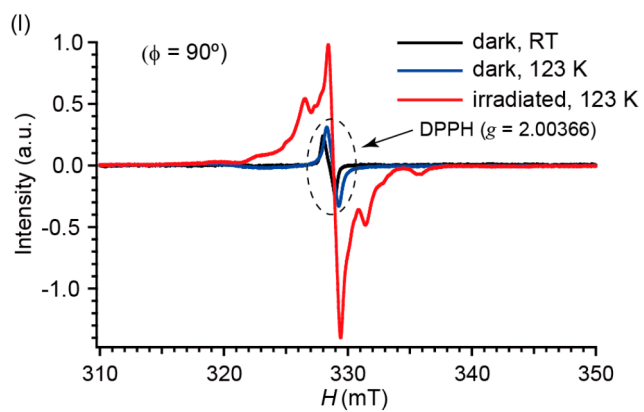
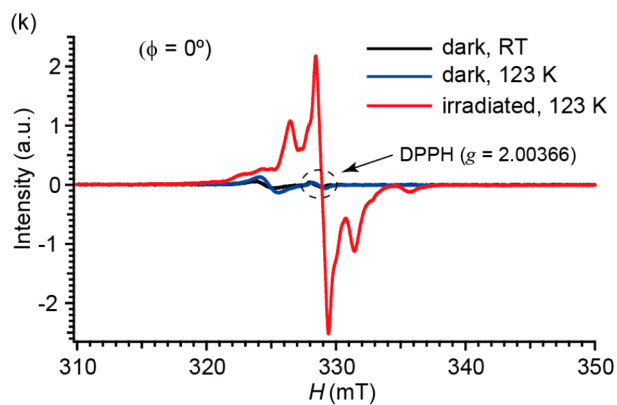
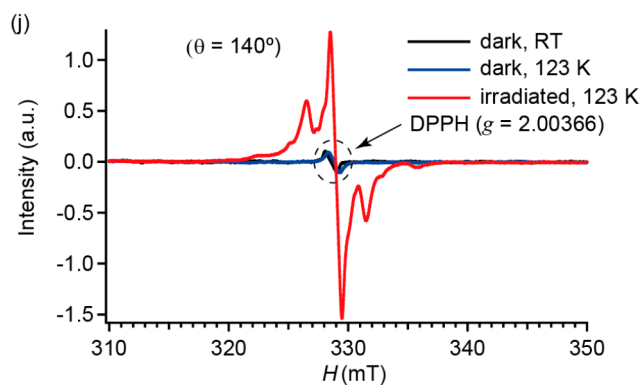
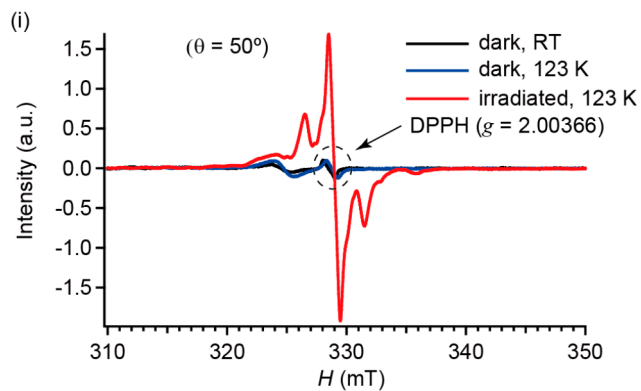
Table S14. Reported principal g -values of $M(\text{dmit})_2$ and related complexes ^{a,b} [72].

Complexes	Host	g_x	g_y	g_z
$[\text{Ni}(\text{mnt})_2]^-$	$[\text{Au}(\text{mnt})_2]^-$	2.042	2.156	1.996
$[\text{Ni}(\text{mnt})_2]^-$	$[\text{Cu}(\text{mnt})_2]^-$ ^c	2.042	2.160	1.998
$[\text{Ni}(\text{dmit})_2]^-$	$[\text{Au}(\text{dmit})_2]^-$	2.041	2.105	2.001
$[\text{Ni}(\text{xdt})_2]^-$	$[\text{Cu}(\text{xdt})_2]^-$	2.045	2.174	2.008
$[\text{Pd}(\text{mnt})_2]^-$	$[\text{Au}(\text{mnt})_2]^-$ ^d	2.043	2.071	1.956
$[\text{Pd}(\text{dmit})_2]^-$	$[\text{Au}(\text{dmit})_2]^-$	2.044	2.045	1.967
$[\text{Pd}(\text{xdt})_2]^-$	$[\text{Cu}(\text{xdt})_2]^-$	2.047	2.069	1.950
$[\text{Pt}(\text{mnt})_2]^-$	$[\text{Au}(\text{mnt})_2]^-$ ^e	2.065	2.245	1.827
$[\text{Pt}(\text{dmit})_2]^-$	$[\text{Au}(\text{dmit})_2]^-$	2.073	2.168	1.858

^a All samples are single crystals of host complexes doped with ~1% of paramagnetic complexes. For the abbreviation and chemical structure of each dithiolene ligand, see below. ^b Experimental errors: $g_i \pm 0.001$ ($i = x, y, z$). ^c Data taken from [77]. ^d Data taken from [78]. ^e Data taken from [79].







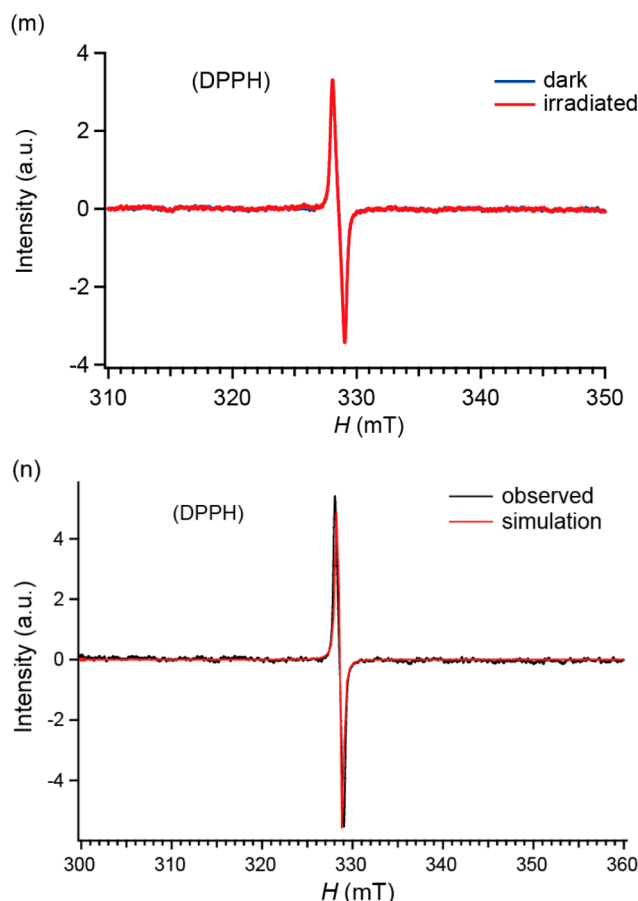


Figure S7. ESR spectra measured with internal standard of DPPH ($g = 2.00366 \pm 0.00004$) under dark and irradiated conditions; for **1**: (a) $\theta = 45^\circ$, the angle expected for minimum g -value under dark conditions; and (b) $\theta = 135^\circ$, the angle expected for maximum g -value under dark conditions. The definition of angle θ is identical with that in Figure 7a. ESR spectra measured with internal standard of DPPH ($g = 2.00366 \pm 0.00004$) under dark and irradiated conditions; for **1**: (c) $\phi = 70^\circ$, the angle expected for minimum g -value under dark conditions; and (d) $\phi = 30^\circ$, an approximate angle expected for maximum g -value under dark conditions. The definition of angle ϕ is identical with that in Figure S8a. ESR spectra of **2** measured with internal standard of DPPH ($g = 2.00366 \pm 0.00004$) under dark and irradiated conditions (e) $\theta = 0^\circ$, the angle expected for minimum g -value under dark conditions; and (f) $\theta = 90^\circ$, the angle expected for maximum g -value under dark conditions. The definition of angle θ is identical with that in Figure 7b. ESR spectra of **2** measured with internal standard of DPPH ($g = 2.00366 \pm 0.00004$) under dark and irradiated conditions (g) $\phi = 90^\circ$, the angle expected for minimum g -value under dark conditions; and (h) $\phi = 0^\circ$, the angle expected for maximum g -value under dark conditions. The definition of angle ϕ is identical with that in Figure S8b. ESR spectra of **3** measured with internal standard of DPPH ($g = 2.00366 \pm 0.00004$) under dark and irradiated conditions: (i) $\theta = 50^\circ$, the angle expected for minimum g -value under dark conditions; and (j) $\theta = 140^\circ$, the angle expected for maximum g -value under dark conditions. The definition of angle θ is identical to that in Figure 7c. For $\theta = 140^\circ$, ESR spectra could be observed only under irradiated conditions. ESR spectra of **3** measured with internal standard of DPPH ($g = 2.00366 \pm 0.00004$) under dark and irradiated conditions: (k) $\phi = 0^\circ$, the angle expected for minimum g -value under dark conditions; and (l) $\phi = 90^\circ$, the angle expected for maximum g -value under dark conditions. The definition of angle ϕ is identical with that in Figure S8c. (m) ESR spectra of the internal standard of a single crystal of DPPH ($g = 2.00366 \pm 0.00004$) under dark and irradiated conditions with a unified intensity scale; the dark and irradiated spectra are completely overlapped. The spectra did not depend on the relative direction of H within experimental error. (n) Comparison of ESR spectra of DPPH between the observed under dark conditions and anisotropically simulated spectrum ($g_x = 2.0045$, $g_y = g_z = 2.0036$, $A_x = A_y = A_z = 0.0001$ (mT) for ^{14}N , $\Gamma_x = \Gamma_y = \Gamma_z = 0.500$ (mT), Lorentzian/Gaussian = 70/30).

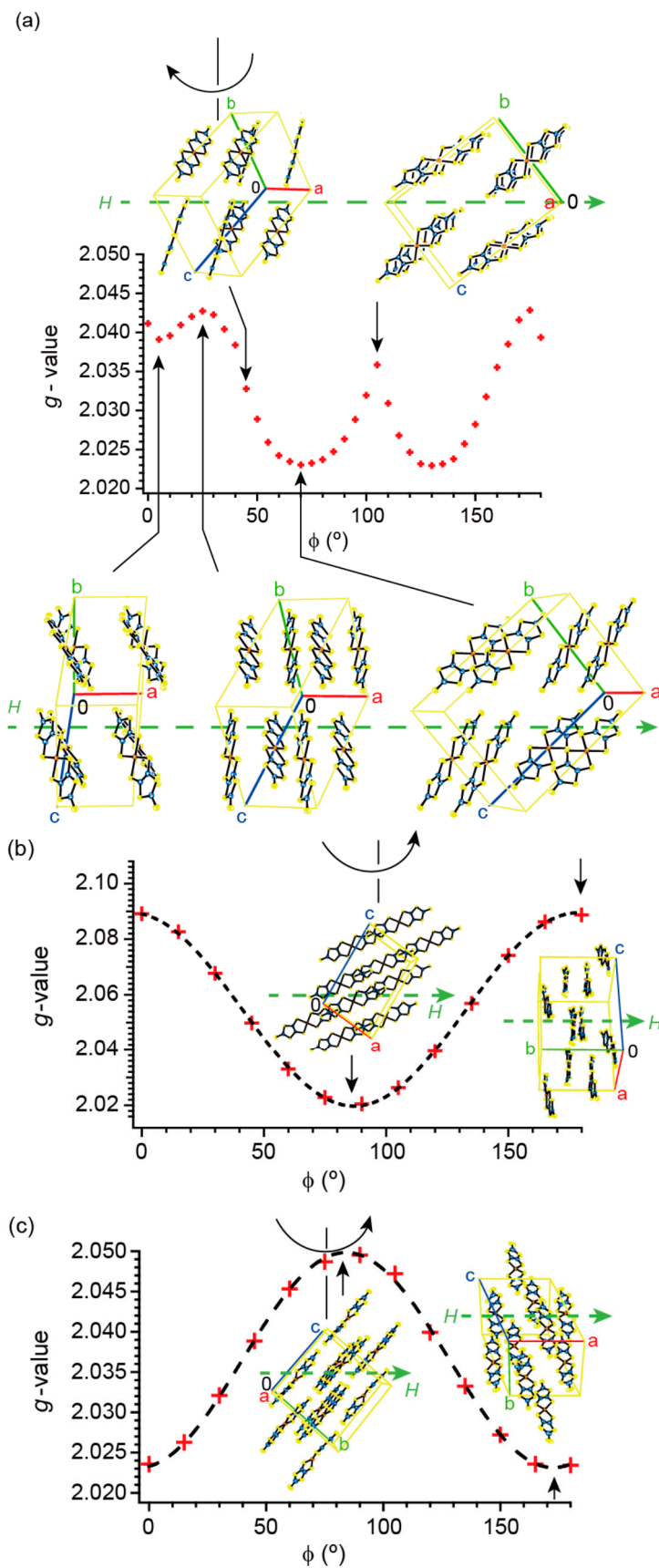
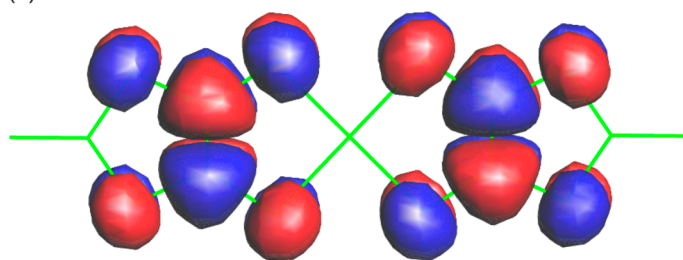
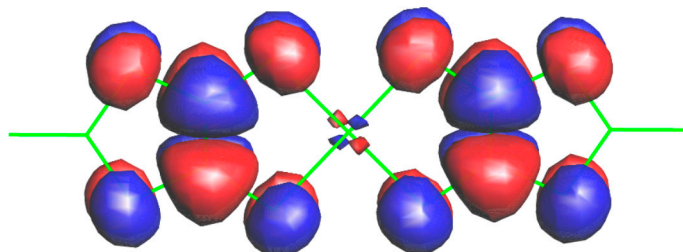


Figure S8. Angle-dependences of g -values (RT, dark) for: (a) 1; (b) 2; and (c) 3. Broken curves are best-fit sine curves in (b) and (c). Note that the rotation axes here are perpendicular to those in Figure 6a–c. The rotation axes are shown in each figure as vertical lines, around which the crystals were rotated in the directions shown by the curved arrows. The molecular orientations relative to H at the maximum and minimum values of g -values are shown in the graphs.

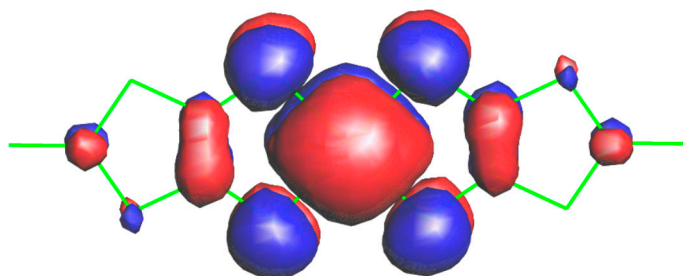
(a)



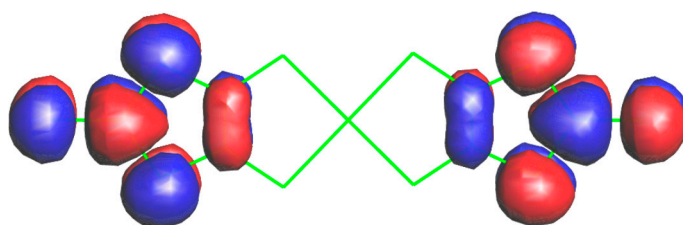
(MO # 54; 5.3 eV = 234 nm)



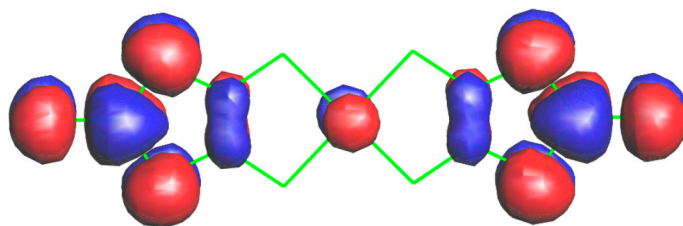
(MO # 53; 5.2 eV = 238 nm)



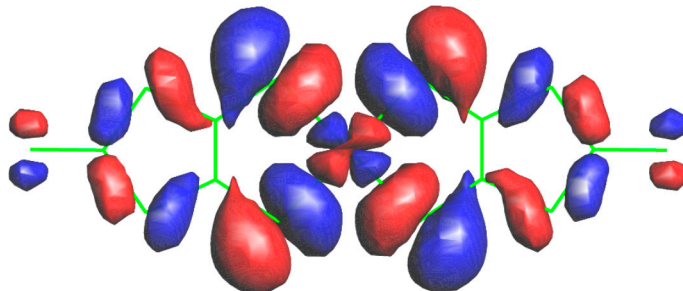
(MO # 52; 4.2 eV = 295 nm)



(MO # 51; 3.2 eV = 388 nm)

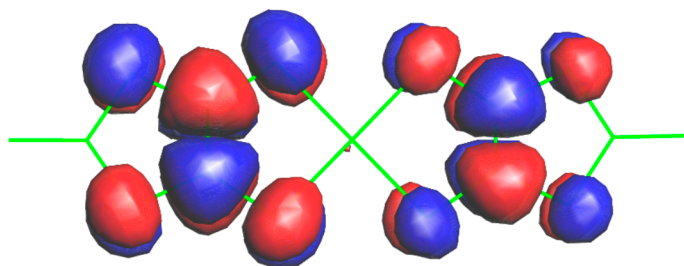


(MO # 50; 3.2 eV = 388 nm)

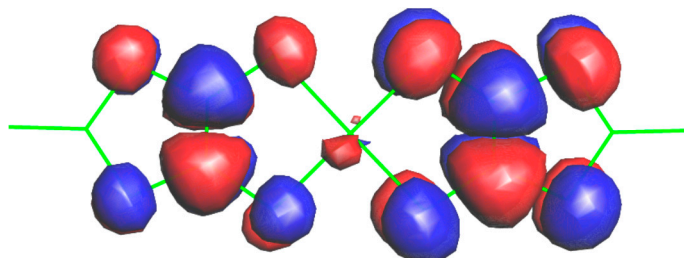


(MO # 49; 0.0 eV)

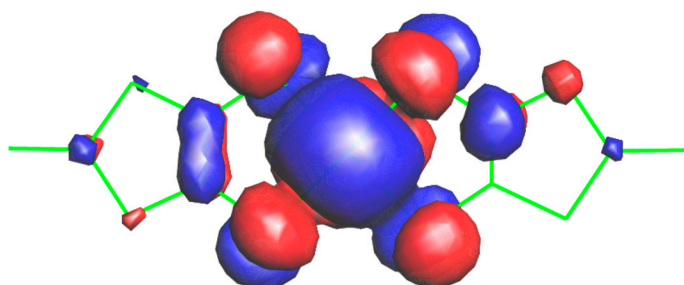
(b)



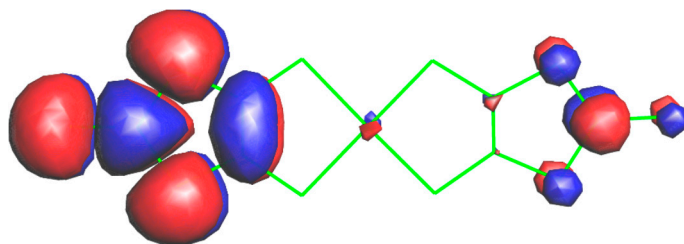
(MO # 54; 5.4 eV = 230 nm)



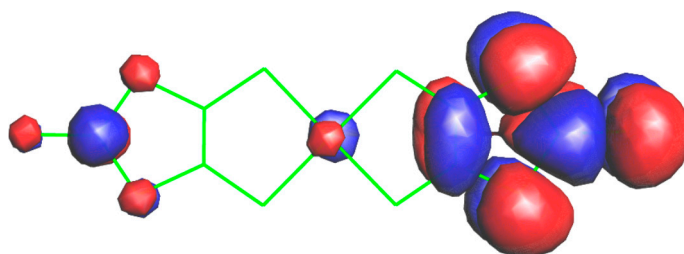
(MO # 53; 5.2 eV = 238 nm)



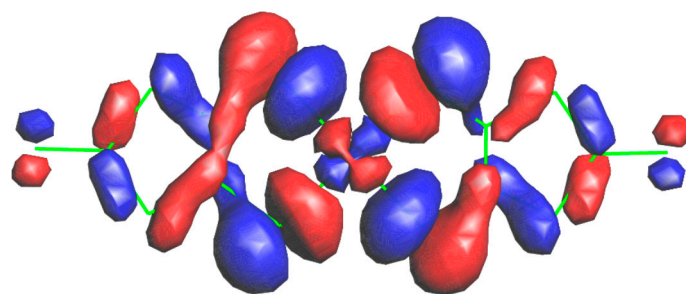
(MO # 52; 4.3 eV = 288 nm)



(MO # 51; 3.3 eV = 376 nm)

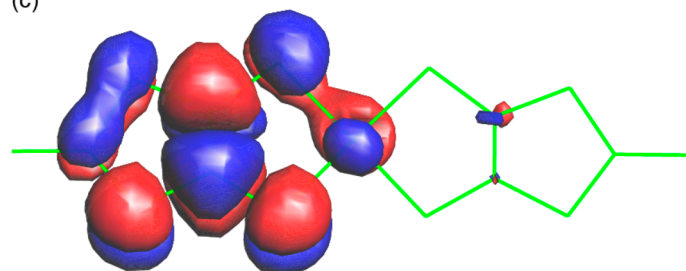


(MO # 50; 3.2 eV = 388 nm)

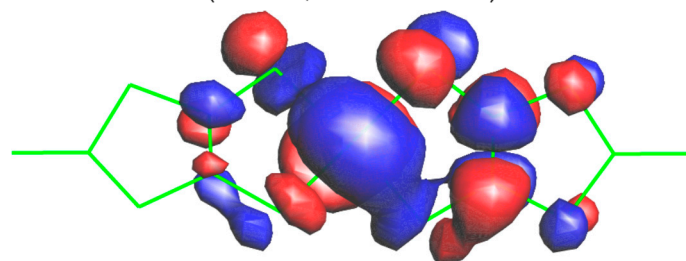


(MO # 49; 0.0 eV)

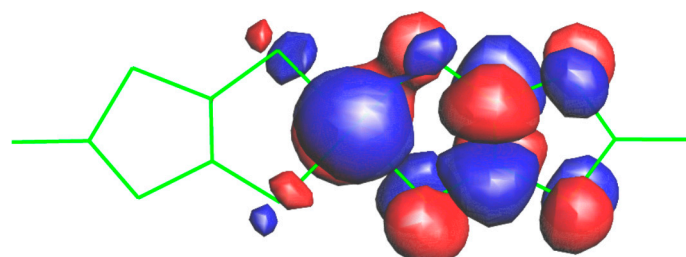
(c)



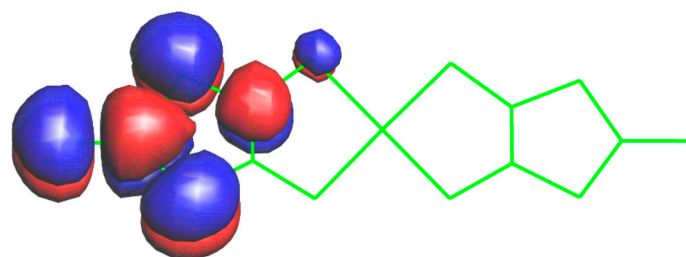
(MO # 54; 5.5 eV = 225 nm)



(MO # 53; 5.5 eV = 225 nm)



(MO # 52; 5.2 eV = 238 nm)



(MO # 51; 3.6 eV = 344 nm)

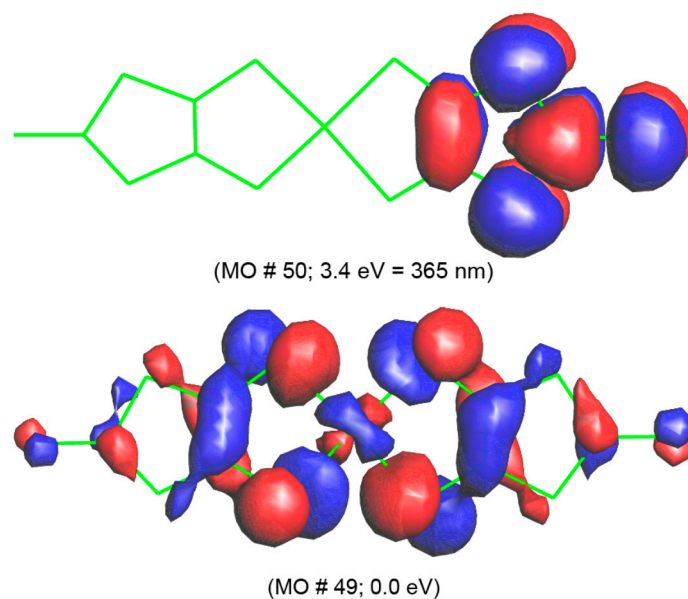


Figure S9. Calculated molecular orbitals for $[\text{Cu}(\text{dmit})_2]^{2-}$; SOMO (MO #49) and those lying around 2.75–5.00 eV (250–450 nm) above the SOMO. Red and blue colors designate different orbital lobes, while green lines designate chemical bonds. (a) MOs from #49–#54 for **1**. The energies are measured from the SOMO (–9.21 eV) based on the extended Hückel calculation; (b) MOs from #49–#54 for **2**. The energies are measured from the SOMO (–9.22 eV) based on the extended Hückel calculation; (c) MOs from #49–#54 for **3**. The energies are measured from the SOMO (–9.45 eV) based on the extended Hückel calculation. The calculation was done by assuming the ground state structures. As the molecular structure of $[\text{Cu}(\text{dmit})_2]^{2-}$ does not alter the MO in a qualitative way (Figure 4), this assumption is valid for qualitative discussion, even if the molecular structures in excited states should be different from those in the ground states.